Developing a Self-Powered, Wireless Damage Detection System for Structural Health Monitoring Applications

by

Luke Andrew Martin

Thesis submitted to the Faculty of Virginia Polytechnic Institute
and State University in partial fulfillment of the requirements for
the degree of

Master of Science

in

Mechanical Engineering

Prof. Daniel J. Inman, Chair
Dr. Moon Kwak
Dr. Yoram Halevi

June, 2004

Center for Intelligent Material Systems and Structures
Blacksburg, Virginia

Keywords: structural health monitoring, piezoelectric, damage detection, impedance, wireless, resonant frequency shift

Developing a Self-Powered, Wireless Damage Detection System for Structural Health Monitoring Applications

Luke Andrew Martin

Abstract

The research presented in this manuscript introduces an independent structural health monitoring (SHM) system capable of performing impedance-based testing and detecting shifts in resonant frequencies. This independent structural health monitoring system incorporates a low power wireless transmitter that sends a warning signal when damage is detected in a structure. Two damage detection techniques were implemented on the SHM system and successfully used for evaluating structural damage. The first impedance-based technique is used to detect a gouge introduced to a composite plate. The second technique is a modal parameter technique that analyzes shifts in natural frequency; this technique was used to detect structural changes in an aluminum cantilever beam. In additional to the above test structures, an aircraft rib provided by the United States Air Force was also tested. This test was performed using the HP 4192A impedance analyzer so that the advantage of high frequency impedance-based tested could be demonstrated.

Insight is given into the power characteristics of SHM systems and the need to incorporate power harvesting into these SHM devices is addressed. Also, a comparison between digital signal processors and microprocessors is included in this document.

Acknowledgements

I would first like to acknowledge Global Contour, GCSB 03-AF0101-0100, for the financial support which made my research possible.

First and foremost, I would like to thank my advisor Professor Daniel J. Inman for making my time with CIMSS and Virginia Tech a delight. In the relatively short time I have known Prof. Inman; I have come to admire his ability to sequentially see the forest and the trees. Studying under an advisor so academically gifted with such a great sensor of humor has been a true pleasure. Without Prof. Inman's support financially, professionally, and personally; none of this would be plausible.

I would also like to think my other committee members Dr. Yoram Halevi and Dr. Moon Kwak for their help. Dr. Kwak's help with some of the details regarding this project help me save valuable time during the course of this research.

Next, I would like to think my mother and father for their love and support. After finishing my Bachelor of Science, they never questioned the decision to further my education by attending graduate school. The fact that they believed in me gave me the confidence I needed to come to Virginia Tech and succeed.

I would like to thank my CIMSS colleagues for putting up with my outrageous stories. The knowledge gained through my colleagues in CIMSS is invaluable.

I would also like to acknowledge the incoming mechanical engineering graduate class of 2002. This group of peers was an exceptional group of individuals who seemed to bond together during our first semester at Virginia Tech. These individuals were always there to lend moral support, to frequent PK's for Tijuana Toss, to tailgate on Saturday mornings, to challenge the mighty New River in a canoe, to visit R.U. when needed, etc. Without this supporting cast of friends, I doubt that graduate school would have been as enjoyable.

Table of Contents

List of Tables

List of Figures

Chapter 1

Introduction

1.1 Introduction to Structural Health Monitoring

Structural health monitoring (SHM) seeks to determine the integrity of a structure using nondestructive techniques. Traditional structural health monitoring can be divided into two major areas: detecting damage within a structure and predicting the location and quantity of damage along with the future life for the structure. Damage is defined, in the SHM community, as a change in the material and/or geometric properties of a structural or mechanical system, including changes to the boundary conditions and system connectivity, which adversely affect current or future performance of that system (Farrar, C. 2003). SHM systems generally compare the current state of the structure with data taken from the past when the state of the structure was known to be healthy. These comparisons to previous states are used to determine whether the structure is damaged or undamaged. Damage detection is always the first goal in any structural health monitoring system. Once a SHM system has identified that damage exists the next steps are to locate and quantify the damage. This process of locating and quantifying damage is computationally challenging since some type of prediction model must be used. This prediction model must locate the damage based on the given information provided by the SHM system, which provides limited data. An adequate prediction model should be capable of quantifying damage within a structure and predicting the future life of the structure. This prediction model is usually based upon a theoretical model of the system; however it is possible to use data from past destructive experiments to estimate damage thresholds for the structure.

In 1993, Rytter proposed a classification system for SHM damage-identification methods. This classification system, originally comprised of four levels, was later

expanded by Inman (2003), who added three levels. These classification levels can be considered the modern structural health monitoring areas of interest. The revised levels for the classification system are as follows:

1. Detect the existence of damage
2. Detect existence and locate damage
3. Detect, locate and quantify damage
4. Detect, locate, quantify and predict remaining life (Prognosis)
5. Combine Level 4 with smart structures to form self-evaluating systems
6. Combine Level 4 with smart structures to form self-healing systems
7. Combine with active control to form simultaneous health monitoring and control

Pearis (2002) successfully incorporated levels one and six of Rytter-Inman's classification system. His research involved the detection of a loose bolt coupled with an shape memory alloy (SMA) actuator to restore the original torque to a bolted joint. Although Pearis' experiment was not coupled with an autonomous system, his research was an attempt to begin filling gaps within this classification system and filling gaps between research and industry.

In recent years, the demand for Structural Health Monitoring (SHM) systems to evolve from inspection and monitoring systems to predictive systems has grown immensely. The demand for SHM systems that have the ability to detect and assess damage has grown from the traditional air/space industry and civil infrastructures to ground transportation, offshore structures, manufacturing machinery, and biomedical devices (Chang 2003). Because of increased industry demand for SHM technology, many conferences and workshops have begun worldwide. The following are a few SHM conferences that were started to expand the technology in this field. In 1997, The First International Workshop on Structural Health Monitoring (IWSHM) was held at Stanford University in Palo Alto, California. In 2002, the First European Workshop on Structural Health Monitoring was held at Ecole Normale Superieure de Cachan in Paris. In

November of 2003, the First International Conference on Structural Health Monitoring and Intelligent Infrastructure was held by the Japan Society of Civil Engineers in Tokyo, Japan.

The future of the structural health monitoring may be better understood by taking a brief look into the history of vibrational analysis in the rotating equipment industry. Since the late 1960's, the rotating equipment field has used vibrational analysis as a diagnostic tool for operational rotating machinery (Ehrich 1999). Until the 1960's, vibrational analysis was primary used by in the development phase to troubleshoot design flaws that would cause undesirable vibration. Today, vibration analysis is a standard practice in industries that use rotating equipment. In general, non-critical equipment, such as pumps and small compressors and their corresponding motors and turbines, are tested once a week or once every two weeks. This testing is performed by a technician who roams the plant with a vibration analyzer and records data for each piece of equipment. This data is stored in the analyzer until it can be downloaded to a database back in the office. The vibration levels of critical equipment are almost always monitored continuously in industry today. Bently-Nevada is a popular manufacturer of such continuous vibration analysis hardware for critical equipment. The vibration analysis hardware is generally programmed to warn the operator that a specific vibration threshold has been reached, considered a level 1 alarm. If the vibration exceeds a threshold where damage to the rotating equipment could occur, the vibration analysis hardware is programmed to shut down this particular piece of rotating equipment.

In the rotating equipment field, health monitoring has become a mature technology. Rotating equipment engineers can analyze vibration data to determine various failures associated with rotating equipment. The following tables extracted from Enrich's "Handbook of Rotordynamics" (Enrich 1999) list malfunctions that can be predicted from changes in the vibration signatures of rotating equipment. These tables are abbreviated for this discussion. Table 1.1 list some equipment malfunctions associated with multiples of the running speed and corrections for these faults.

Table 1.1. Malfunctions associated with harmonic frequencies

Fault	Frequency	Spectrum, time domain, orbit shape	Correction
Mass unbalance	1X = one times running speed	Distinct 1X with much lower values of 2X, 3X, etc., elliptical and circular orbits	Field or shop balancing
Misalignment	1X, 2X, etc.	Distinct 1X with equal or higher values of 2X, 3X, etc., figure-eight orbit	Perform hot and/or cold alignment
Shaft bow	1X	Dropout of Vibration around critical speed in Bode plot	Heating or peening to straighten rotor
Bearing wear	1X, subharmonics, orders	High 1X, high ½ X, sometimes 1½ X or orders; cannot be balanced	Replace bearing

In addition malfunctions that excite synchronous frequencies, subsynchronous excitations are often an indication of a malfunction as well. Table 1.2 is a brief excerpt from Ehrich of predicted malfunctions that result in subsynchronous excitations.

Table 1.2. Malfunctions associated with subharmonic frequencies

Fault	Frequency	Spectrum, time domain, orbit shape	Correction
Oil whirl	0.35X to 0.47X	Subsynchronous component less than ½ order informal loop in orbit	Temporary: load bearing heavier, correct misalignment; Longterm: change bearing type
Subharmonic resonance	1/2 X, 1/3 X, ¼ X, and higher	Subsynchronous vibration depending on natural frequency	Remove looseness, excessive flexibility; change natural frequency so that it does not match fractional frequencies
Rubs	1/2 X, 1/3 X, ¼ X, and higher	External loops in orbit	Eliminate condition such as thermal bow and mass unbalance that causes rub

Tables 1.1 and 1.2 give an idea of the failure modes that can be detected in the rotating equipment field. Obviously these failure modes are unrelated to structural health monitoring, however they should be used to enlighten about the diagnostic usefulness of vibration data in engineering.

A recent trend in the rotating equipment industry has been to change from preventive maintenance to predictive maintenance techniques. Preventive maintenance encompasses the old school methodology of periodically removing a piece of equipment from service and performing the necessary routine maintenance. The shift to predictive maintenance has emerged in recent years mainly due to advances in computing technology. These advances have made portable vibration analyzers practical tool for

day to day use. Companies are shifting to predictive techniques to reduce maintenance cost.

This paradigm shift from preventive maintenance to predictive maintenance is now desired by many new industries. However, instead of evaluating rotating systems these industries are interested in the capability of evaluating structural systems, hence the introduction of structural health monitoring.

1.2 Literature Review

The following sections will discuss current technology in the area of structural health monitoring. A background of theoretical damage detection methods will be given in the first section. The second section will discuss SHM systems that have been developed. In this discussion, the argument over power consumption and whether data computation should be performed at the sensor and transmitter location or at the central computer and receiver location will be addressed. These sections should serve as a brief overview of some common topics within the field.

1.2.1 Damage Detection Methods

The resonant frequency shift method is probably the most intuitive vibration method used to detect damage in a structure. For a single degree of freedom system, from elementary vibrations, the natural frequency is

$$\omega_n = \sqrt{\frac{k}{m}} \tag{1.1}$$

where k is the stiffness and m is the mass. Generally, the goal of this method is to detect a change in stiffness of the structure, since the mass is assumed constant. This change in frequency will appear in the frequency response function (FRF) as a decrease in resonant

frequency. This method is capable of detecting global changes within a structure and can be classified as one of the three basic modal parameter methods. The other two modal parameter methods are change in mode shapes and changes in modal damping (Salawu 1997). Salawu (1997) states that in literature, the terms natural frequency, modal frequency, and resonant frequency refer to the same item. This thesis will use the term resonant frequency from this point to avoid confusion. Although Salawu's 1997 paper does not present the mathematical background for resonant frequency changes, his paper is an excellent review of damage diagnostics using resonant frequency changes. In addition, only resonant frequency shifts and change in mode shapes will be discussed in this literature review. The most significant drawback of the resonant frequency shift method is its low sensitivity to damage, which requires very precise measurements or large levels of damage (Doebling, et al. 1998). On the contrary, the resonant frequency shift method exhibits less statistical variation from random error sources than other modal parameter methods (Farrar, et al. (1997), Doebling, et al. (1997)).

The mode shape method is another modal parameter method used to detect damage within a structure. Using the modal assurance criterion (MAC) to correlate between modes, West (1984) presented, for the first time, a way to detect and locate damage in a structure without using a prior finite element modal (FEM). Since this time, researchers have showed that damage detection algorithms can be used to identify damage from measured data without the aid of finite element models. The major downfall of the mode shape method is the large number of sensors needed to gather enough data to accurately identify modes. In simulated results, mode shape changes are more sensitive to damage than the resonant frequency method. However, due to lack of accuracy in experimentally identified modes these simulated results are difficult to verify (Park 2000). Doebling (1997) showed that resonant frequencies are less difficult to obtain than mode shapes.

The major limitation of modal parameter methods is their inability to detect damage at a local level. These methods utilize lower-order global modes which are

insensitive to local changes in the structure; the use of these methods may result in the detection of damage slightly before catastrophic failure.

Recent research has shown that Lamb wave propagation methods have future potential for practical use since experimental results show that local damage can readily be detected. The basic theory is that a Lamb wave will be transmitted from a piezoelectric (PZT) actuator to a piezoelectric sensor. The undamaged case will set the baseline and when damage is present changes will occur in the transmission velocity and wave reflections. This damage also gives valuable insight into the type of damage that has been detected. Through cracks and surface cracks can be detected independently, in monolithic materials, using Lamb wave propagation methods. In laminate materials, embedded delamination and surface delamination can be detected independently using Lamb wave propagation. In general, Lamb waves excite two modes within the structure; these modes are asymmetric and symmetric. The asymmetric mode is sensitive to surface damage while the symmetric mode is sensitive to through-thickness irregularities (Park, et al. 2003).

Impedance-based structural health monitoring techniques were founded on the electromechanical coupling property of piezoelectric materials. When a piezoelectric material, most commonly a wafer, is bonded to a structure the electrical impedance of the wafer is related to the mechanical impedance of the structure. In a finite element sense, this mechanical impedance can be thought of as the mass and stiffness matrices. In practice the mechanical impedance is related to the mass, stiffness, and damping of a structure. When damage is introduced to a structure the mechanical impedance will change, hence the electrical impedance will also change.

Figure 1.1 illustrates the 1-D model used to describe the coupling between electrical and mechanical impedance. In the PZT-driven dynamic structural system depicted in Figure 1.1, the PZT is a thin bar that vibrates in the axial direction due to the applied alternating voltage.

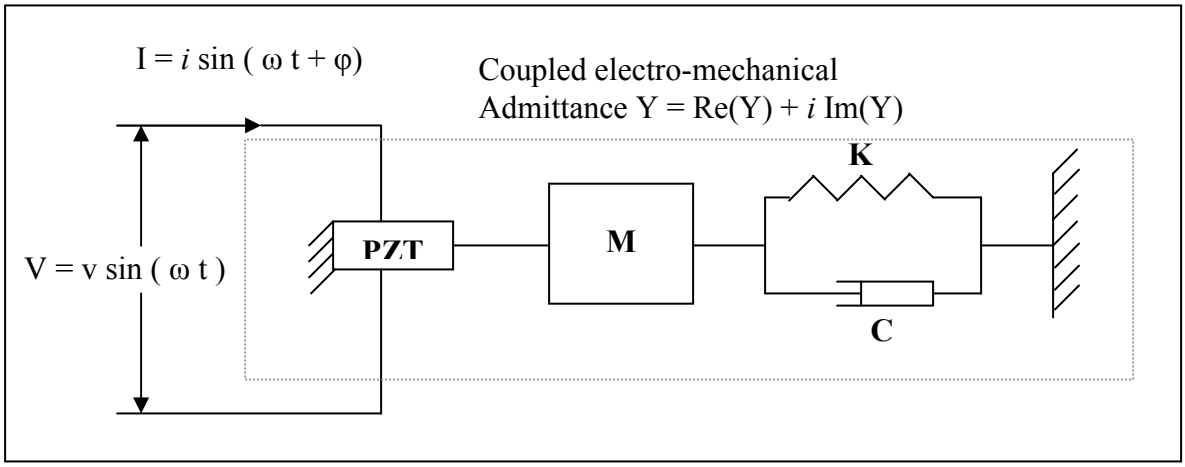

Figure 1.1. 1-D model representing a PZT-driven dynamic structural system

The wave equation is then solved for the PZT bar connected to the structure. The solution relates the frequency to the electrical admittance (Liang *et al*. 1994) and is given by:

$$Y(\omega) = i\omega a\left(\bar{\varepsilon}_{33}^{T}(1-i\delta) - \frac{Z_s(\omega)}{Z_s(\omega)+Z_a(\omega)} d_{3x}^{2}\hat{Y}_{xx}^{E}\right) \tag{1.2}$$

In equation 1.2, Y is the electrical admittance, Z_a is the PZT material's mechanical impedance, Z_s is the structure's mechanical impedance, $\hat{Y}_{xx}^{E}$ is the complex Young's modulus of the PZT with zero electric field, $\bar{\varepsilon}_{33}^{T}$ is the dielectric constant at zero stress, d_{3x} is the piezoelectric coupling constant in the arbitrary x direction at zero stress, δ is the dielectric loss tangent of the PZT, and a is the geometric constant of the PZT (Park 2000). This change in electrical admittance is inversely proportional to electrical impedance, which can be measured with an impedance analyzer. Gyuhae Park's dissertation should be referred to for a more detailed description of this method and experiments performed using this method (Park 2000).

Damage Detection using Instantaneous Phase Features is a new approach that uses a structural-wave-phase relationship to infer damage (Salvino 2003). The idea here is that structural damage will alter the speed that energy waves travel through a structure. An instantaneous phase function, relative to some reference point on the structure, is defined to represent the phase of these traveling waves. When damage is introduced to the structure, the rate at which energy waves travel through the structure will decrease resulting in a phase delay. It has been shown that this method is effective in identifying and locating damage within a structure. Salvino's paper should be referred to for a more complete explanation of this method.

This section aims to serve as an abbreviated summary of past and present damage detection techniques used in structural health monitoring applications. An excellent paper dealing with vibration based damage detection methods is (Doebling 1998). For additional information regarding vibration and non-vibration based techniques refer to the diagnostic section of the *Proceeding of the 4th International Workshop on Structural Health Monitoring*.

1.2.2 Structural Health Monitoring Systems

Although structural health monitoring technology is still in a prototype phase, researchers have begun to implement stand alone SHM systems. This section will discuss some systems that have been developed and also allude to debates about how these systems should operate.

Trego (2003) has developed and implemented a prototype autonomous structural integrity system (ASIMS) that monitors corrosive environments on a Delta Air Lines 767. This system uses sensors to monitor moisture, relative humidity, temperature, pressure and static strain measurements. Corrosion is a principle maintenance expense in ageing aircraft. The main acquisition board uses a microprocessor to control the system and process sensor data. After the sensor data is processed, the processed data is stored in non-volatile flash memory and can later be downloaded to a PC via a serial port. The

operations of the main acquisition board can also be modified through this serial port. This acquisition board has eight analog channels that are capable of sampling at 10 kHz. Power consumption is less than 1.5 watts, during data acquisition. The ASIMS requires a DC power supply of between 8 V to 40 V and a standby current of less than 300 mA. Non-rechargeable D2/3A cell batteries are used as the power supply. This prototype SHM system is one of the few examples of a system that has been implemented on a commercial vehicle.

Structural health monitoring systems are also being considered to study the affect of seismic events on structures. Çelebi (2003) presents a seismic monitoring system for a 24-story building. In near real time, this system records accelerations then computes displacements and drift ratios. Structural engineers can use drift ratios to access the damage condition of a building. However, this system is capable of interpreting the drift ratios and alerting occupants of the buildings current structural status. Çelebi suggest the use of three status levels "green = unrestricted use of structure", "yellow = structure only to be accessed for emergency reasons", and "red = structure is unsafe for entry". A PC is used to monitoring a constant stream of acceleration data for thirty accelerometers. When acceleration thresholds are surpassed, the PC records data and stores this data within the building and/or to a remote location via high-speed internet.

Lynch (2003b) introduces one of the first wireless sensing units capable of evaluating SHM algorithms. His system would operate by collecting data from sensors and then processing this data at the sensor location. After this data is processed a wireless signal would be transmitted indicating the health of the structure. For his application, two microcontrollers were researched the first a Atmel AVR AT90S8515 and the second a Motorola MPC555. The AVR microcontroller presented excellent energy characteristics only drawing 8 mA of current at 5 Volts or 0.04 Watts of power. However, this 8-bit system did not have sufficient internal memory storage to run the complex SHM algorithms. The MPC555 microcontroller was then investigated. This 32-bit microcontroller has the sufficient internal memory to run the SHM algorithms. Although, the major draw back of the MPC555 microcontroller in comparison to the

Atmel AVR microcontroller is that the MPC555 draws 110 mA of current from a 3.3 Volt source or 0.33 Watts of power. However, in practice this system would remain off until activated by an external trigger when scheduled testing was to be preformed. Performing computations at the sensor location is a new school of thought that Lynch refers to as a paradigm-shift. While the old school of thought was to transmit all collected data and perform computations at some central processing unit. Energy savings is the key reason for this change in philosophy. Lynch's (2003c) energy analysis that compared data interrogation versus transmission demonstrated the validity of this philosophy. The results of his analysis showed that the energy consumed by a MPC555 for FFT calculations were 0.0152 J, 0.0328 J, and 0.0702 J for data of length 1024, 2048, and 4096, respectively. His analysis suggests that the processing speed of the MPC555 was in the range of 21 kHz to 25 kHz.

Lynch's utilized a Proxim RangeLAN2 7911 wireless modem as the wireless transmission device. This wireless modem draws during transmission periods 190 mA and 60 mA when idle from a 5 Volt source, which translates to 0.95 Watts and 0.03 Watts, respectively. The range for this modem is 1,000 feet (305 meters) in open areas and 500 feet (152 meters) within a building.

Sazonov (2004) presents a Wireless Intelligent Sensor and Actuator Network (WISAN) that can serve as an autonomous structural health monitoring system. This WISAN system exhibits very low power consumption characteristics in comparison to other SHM systems. The system can exhibit such low power characteristics because it does not perform onboard computing and also the system does not rely on active sensing. The total power requirement is 75 mW at 3 Volts. However, the WISAN continuously samples and transmits data. The cumulative energy required to operate this system far exceeds that of SHM systems that sample and transmit at periodic intervals. Sazonov claims that computational capabilities at the sensor location are an unjustified uses of energy. The other school of thought is to perform all computations at the sensor location and then only transmit a warning signal to an operator's panel. This debate, which is the key difference between Lynch's and Sazonov's research, has not been settled. In the

author's opinion, as will be shown later in this thesis, wireless transmission of a warning signal is more energy efficient than a continuous transmission of data, as proposed by Sazonov's method. However, future research should be to minimize the power consumption of computational chip circuits. For this thesis, minimizing these circuits was unpractical since specialized computational chip circuits could not be utilized do to constant algorithm modification during the course of the research project.

1.3 Research Objectives

The objective of this research was to construct a structural health monitoring system that would use lead-zirconate-titanate patches (PZT) as sensors and actuators, incorporate power harvesting, detect damage in a structure, include a wireless telemetry system and perform computing at the sensor location. This SHM system would be capable of damage detection. Two major areas of concern arouse when planning the research: one was the computing system and how it would be programmed and the other was the basic theory to be used for the SHM algorithm. Because of the need to build multiply algorithms and continuously improve these algorithms, research time was devoted to algorithm development. An off the self PC 104 board was purchased and implemented, allowing research time to be concentrated on the development of the SHM algorithms needed to detect damage. The first damage detection algorithm implemented is based on simple vibration theory, this allowed for more time to be spent learning about computing systems and data acquisition. The other damage detection algorithm implemented utilized the impedance method. Another area of research to be performed was a power consumption audit of all components used. This would allow future researchers to easily begin optimizing the power consumption of the system.

1.4 Overview of CIMSS Structural Health Monitoring System

This section will briefly present the Structural Health Monitoring System developed by CIMSS and its components. Throughout the remainder of this system will be referred to as the CIMSS Structural Health Monitoring System or CSHMS.

This research has been broken in four major areas of research. These areas are power harvesting, chip computing, damage detection technique, and telemetry. In addition, chip computing can be further broken into the following areas, data acquisition and processing. Figure 1.2 is a schematic overview of the CIMSS Structural Health Monitoring System (CSHMS). An overview of the CSHMS is given in the following paragraph.

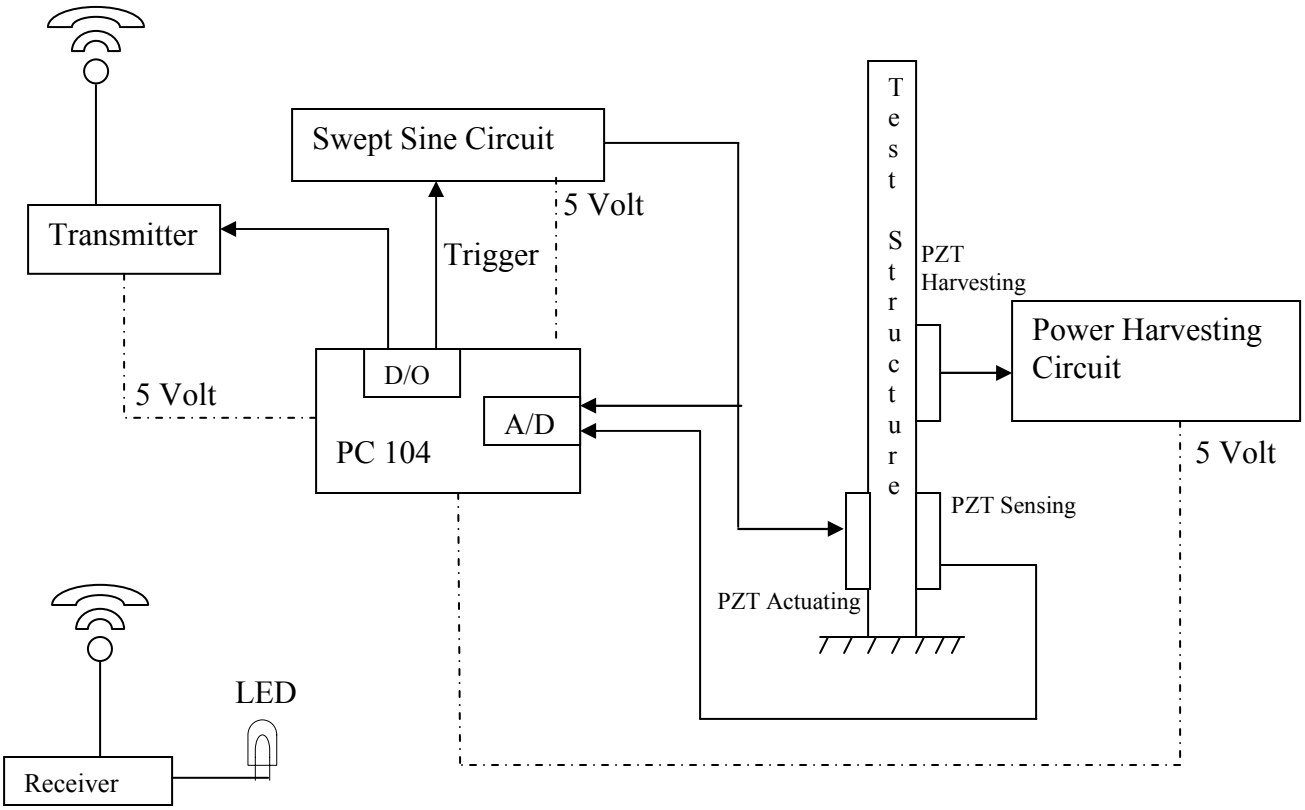

Figure 1.2. Schematic of CIMSS Structural Health Monitoring System (CSHMS)

In application, the PC 104 board would be programmed on a sleep timer to awake and test the structure at periodic intervals. The time between intervals is application specific. Two important factors to consider when setting a time interval for testing are: 1) how often the needed power will be available and 2) how fast the structure deteriorates. Another alternate is to trigger the PC 104 to awake after a catastrophic event has occurred

in the structure. Once the PC 104 board is awaked from standby, it outputs a digital trigger signal to the swept sine circuit which sends out an excitation signal to the actuating PZT. The signal sent to the actuating PZT and the response from the sensing PZT would be sampled using the A/D converters on the PC 104 board. The PC 104 board would then compute the Fast Fourier Transform (FFT) of each signal and then compute the frequency response function (FRF). Depending on the damage detection technique, the magnitude of the FRF or the real part of the FRF will be further examined and compared to a baseline FRF to determine if damage has occurred in the structure. If damage is detected then the PC 104 board will output a digital signal to the transmitter. The receiver will collect this signal and send the appropriate warning signal. For demonstration purposes, when no damage was detected the LED is illuminated and when damage was detected the LED blinks. The system will then return to standby mode until the next testing time. A battery is charged, in the power harvesting circuit, from ambient vibrations of the structure during standby mode.

Figure 1.2 depicts the configuration of the SHM system for the vibration based damage detection technique. For the impedance-based technique the low cost circuit is added to the system and only one PZT is needed for both sensing and actuating. The low cost circuit is added so that impedance can be measured. The real part of this impedance measurement is used to detect damage in the structure.

1.5 Research Contributions

The major contribution of this research was a miniaturized system that is capable of taking impedance measurements. In addition to recording impedance measurement, the CIMSS Structural Health Monitoring System developed also analyzes the recorded data and outputs a wireless signal indicating the health of the structure.

Another contribution of this research is related to the power requirements of the CSHMS developed. Although the CSHMS developed does not exhibit the lowest instantaneous power requirement, the concept of periodic sampling coupled with the

previously mentioned power harvesting makes this system more efficient over the sampling period than prior systems. This idea of only needing to power a timer during idle periods should make CSHMS more desirable for practical applications.

1.6 Thesis Overview

The major aspects involved with the development of a practical structural health monitoring system are addressed in this thesis. The goals of the CSHMS were to transmit a wireless warning signal, utilize power harvesting, detect damage using a vibration based algorithm, and incorporate a microcomputer to perform computing at the sensor location.

Wireless transmission and reception will be discussed in chapter 2. This chapter will begin with an overview of the importance of wireless technology in structural health monitoring systems. Next, the transmitter and receiver used for our application will be discussed in detail. Finally, an energy audit of these components will be reported along with a comparison to other wireless systems using in SHM systems.

The components of the CIMSS SHM system are the subject of chapter 3. PC/104 boards are introduced and the specifications of the PC/104 board used for testing are given. Next, the low cost method is discussed as a way of measuring impedance without the need for an impedance analyzer. Then power harvesting is introduced and the benefits of building a SHM system that is capable of power harvesting are given. A proposed power harvesting circuit is suggested in this section. Finally, the advantages of digital signal processors when compared to microprocessors are discussed.

The focus of chapter 4 is results obtained from two damage detection techniques. Many different techniques were discussed in the literature review; however, this chapter will concentrate on the impedance method and the resonant frequency shift method. For the impedance method, experimental results from a composite plate and aircraft rib will

be presented. Next, results from the resonant frequency shift method applied to an aluminum cantilever beam with variable mass will be presented.

Finally, a summary of the research presented will be given in chapter 5. The contributions this research has made to the Structural Health Monitoring community will be given. Then the future work to be conducted on the CSHMS and in the area of structural health monitoring systems in general will be present.

Chapter 2

Wireless Transmitter and Receiver

2.1 Introduction to Wireless Communication

Wireless communication is an important field of structural health monitoring. Wireless SHM systems are favored over wired systems for numerous reasons. A few of these reasons are they reduce installation cost, are less likely to corrupt data, and eliminate the need to repair or replace wires. An example of the need for wireless SHM systems comes from a California state law that declares every new structure over six stories or 59,000 ft^2 must be implemented with a SHM system. The cost for such a system can be greatly reduced if wireless technology is used (Lynch 2002).

The common approach when purposing wireless SHM systems is to collect data from a sensor and then transfer this raw data wirelessly to a central computing unit for additional processing. However, processing the raw data at the sensor location and sending a signal solely about the state of the structure will consume less power than wirelessly transmitting all of the raw data to a central computing unit. The wireless signal transmitted will only indicate the state of the structure. For the first stage of our study, the state of the structure is simply yes damage exist (red light) or no damage exist (green light). In future applications, encoders and decoders can be added to the current wireless configuration to allow for encrypted wireless serial communication. This additional hardware will give the system the ability to indicate how much damage has occurred within the structure. For example, instead of stating yes damage has occurred we would now be able to state 20% or 50% damage has occurred in the structure. Ultimately, we would like to be capable of predicting future life based on design loading cases or past loading scenarios.

2.2 Wireless Data Transfer using Radiometrix Telemetry Devices

To meet our expectations in the first stage, a wireless telemetry system needed to be implemented. The main objective of this system, although capable of serial communication, was to transmit a yes or no indication about whether damage had occurred or not. The products we choose, to achieve this objective, were Radiometrix UHF FM Data Transmitter and Receiver Modules. These modules were mainly chosen because of their small size (less than 2" x 1/8" x 1/2") and low power requirements (transmitter power is 47.2 mW), which will be discussed in further detail in the following sections. Because of their power characteristics, these modules are an excellent choice for a battery powered application. Also, these modules were relatively inexpensive in comparison to the entire cost of the SHM system. The Radiometrix designation for the transmitter and receiver are TX-2 and RX-2, respectively. The following sections explain how to use these modules, gives OEM schematics, module specifications and includes some laboratory photographs for each module. The schematics shown are available for consumers use at www.radiometrix.com.

2.2.1 The Radiometrix Transmitter (TX-2)

A Radiometrix TX-2-433-40-5V transmitter was used for our application. This transmitter is capable of sending data at a rate of 160 kbps. The transmitter's useable range is up to 300 meters for open ground and 75 meters in a building. The transmission frequency is 422.92 MHz. Figure 2.1 below illustrates the internal components of the TX-2 transmitter. As seen in Figure 2.1, the data passes through a low-pass filter before being transmitted.

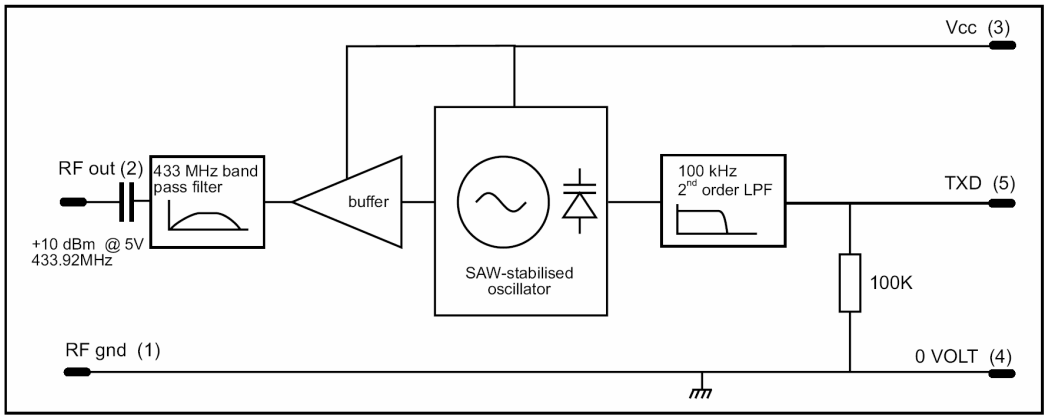

Figure 2.1. Internal components of TX-2 module

Figure 2.2 is an external schematic of the TX-2 transmitter. This figure can be used to properly wire the transmitter. A supply voltage of 4.0 V to 6.0 V is needed for the transmitter module. The supply current ranges from a minimum of 7 mA to a maximum of 14 mA. The transmitter's nominal power demand is 50 mW with an absolute minimum and maximum of 28 mW to 84 mW, respectively.

After integrating the transmitter into our SHM system, a power audit was preformed to narrow the transmitter power range. The transmitter draws a current of 9.31 ± 0.015 mA from a supply voltage of 5.07 V. The transmitter's power demand for the SHM system is 47.2 ± 0.077 mW. The power requirement stated here is transmitting power the standby power requirement is zero since there is no need to use the transmitter when the SHM system is on standby.

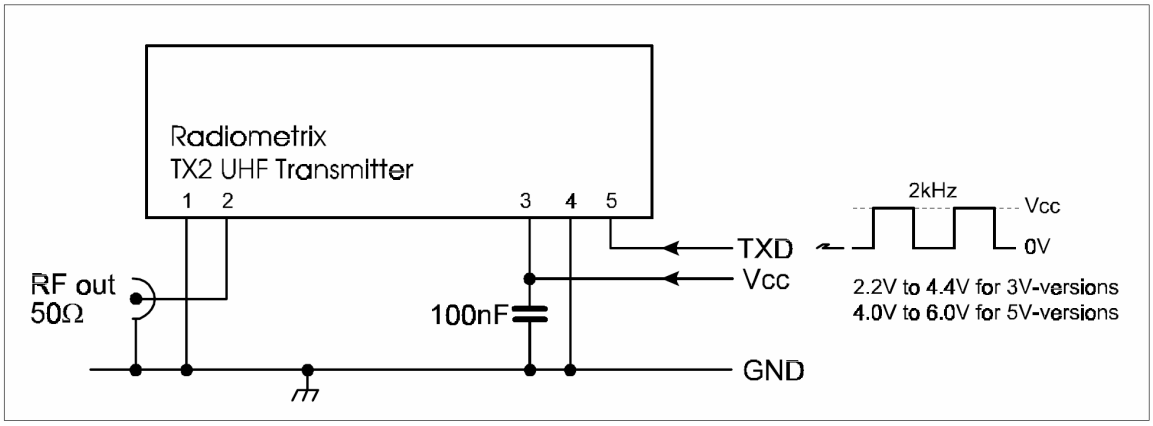

Figure 2.2. External schmatic of TX-2

Figure 2.3 is a picture of the TX-2 transmitter used in laboratory experiments. The dimensions of the transmitter are 1.25” long by 1/8” wide by 7/16” high. The only additional components that need to be added to complete the transmitter circuit are a 100 nF capacitor, a 15.5 cm long wire antenna, and any wires or soldered connections for the power supply.

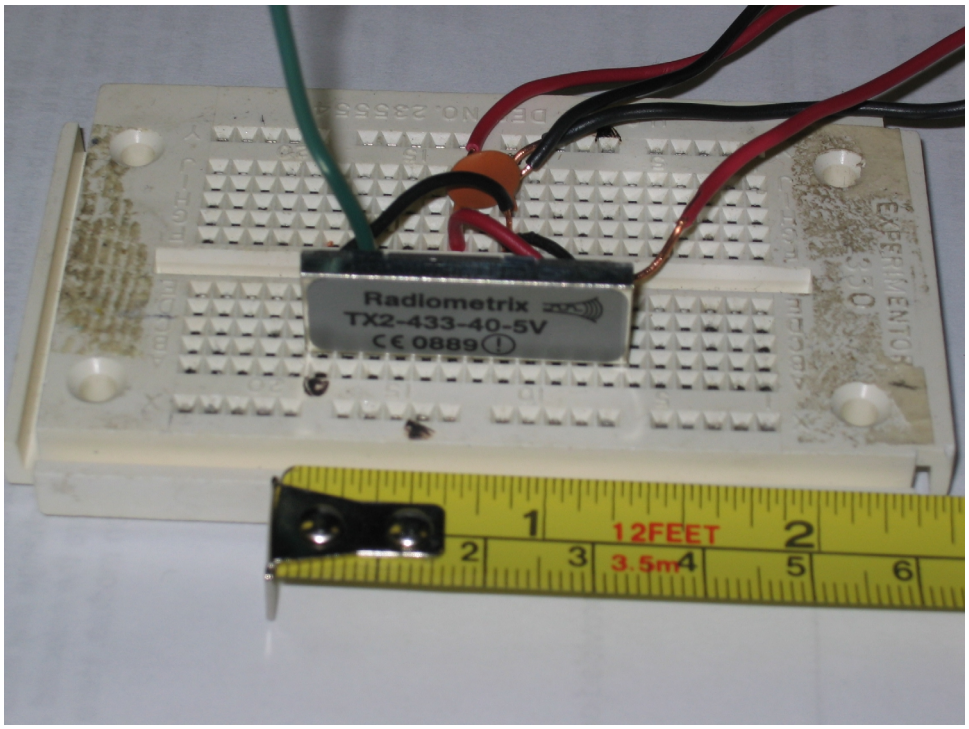

Figure 2.3. Radiometrix TX-2 transmitter used in laboratory experiment

2.2.2 The Radiometrix Receiver (RX-2)

The Radiometrix RX-2-433-40-5V receiver used for our application is illustrated in Figure 2.4. A supply voltage of 4.0 V to 6.0 V is needed for the receiver module. The current demand ranges between 11 mA to 17 mA. However, the nominal power demands of the receiver are not of great importance since the receiver does not draw its power from our power harvesting circuit.

Although the receiver power requirements are not of great importance to the overall power scheme of the SHM system, they are include here for completeness. The

power audit performed after integrating the receiver into our SHM system yielded a receiver demand of 15.38 ± 0.035 mA from a supply voltage of 5.00 V. The resulting power demand of the receiver is 76.88 ± 0.176 mW.

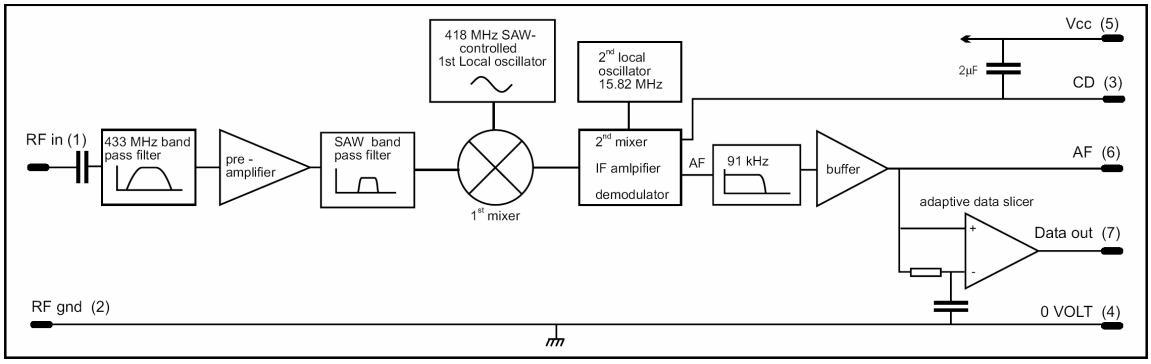

Figure 2.4. Internal components of RX-2 module

Figure 2.5 is an external schematic of the RX-2 receiver.

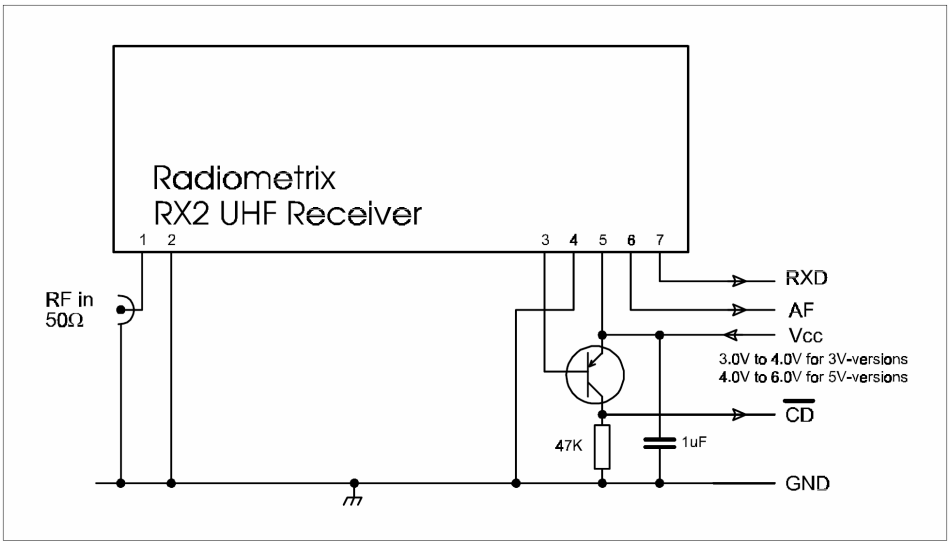

Figure 2.5. External schematic of RX-2

Figure 2.6 is a picture of the RX-2 receiver used in laboratory experiments. Notice in the clear LED in Figure 2.6. This LED is red (on) when damage has occurred and is clear (off) when no damage has occurred. The dimensions of the receiver are 1-12/16" long by 1/8" wide by 7/16" high. In addition to the receiver, the following

components are needed to complete the receiving circuit: a 15.5 cm wire antenna, a LED, a resistor in series with the LED, and the needed wires for the power supply.

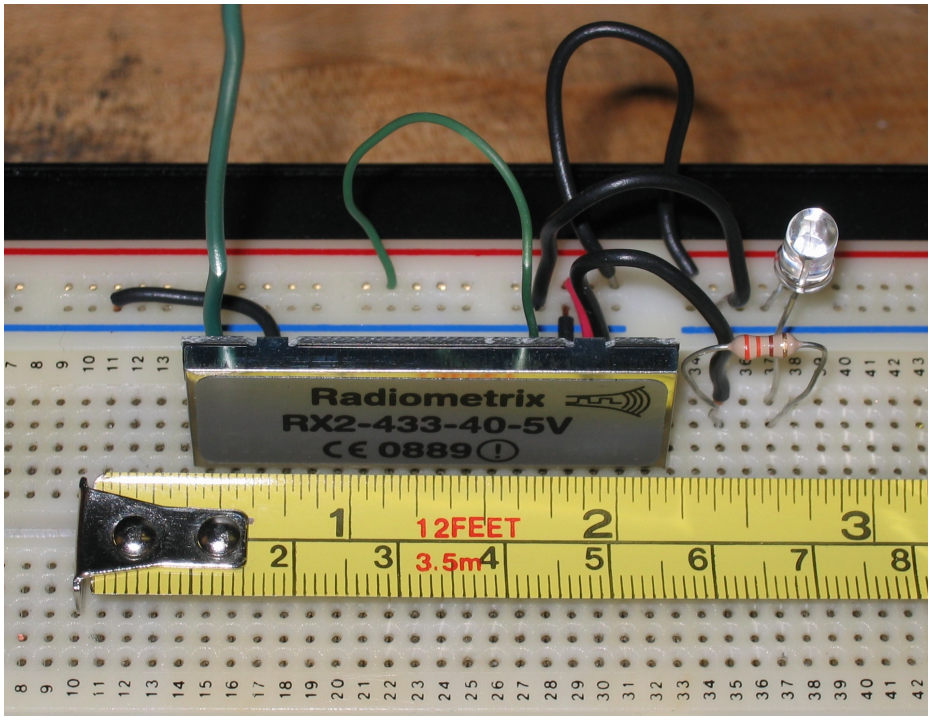

Figure 2.6. Radiometrix RX2 receiver using in laboratory experiments

2.2.3 Antenna Considerations

Another area of interest was the type of antenna used to transmit the wireless indication signal. Radiometrix suggests three antenna configurations for their TX2/RX2 line of transmitters and receivers. The three antenna configurations are helical, loop, and wire.

For the helical antenna shown in Figure 2.7, Radiometrix recommends using a 0.5 mm enameled copper wire. This wire should then be wound 24 turns on a 2.2 mm diameter rod. The major advantage of the helical configuration as opposed to the other two is its size. The open ground range for this configuration is 300 meters.

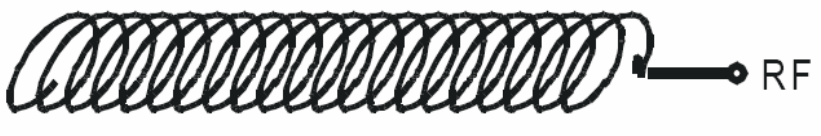

Figure 2.7. Helical antenna suggested by Radiometrix

The loop antenna, shown in Figure 2.8, is the hardest of the three configurations to build. Four capacitors are needed for this design, which offers the best immunity to noise of the three antennas. The area enclosed by the loop should by between 4 and 10 cm^2. The open ground range for the loop antenna is only 100 meters.

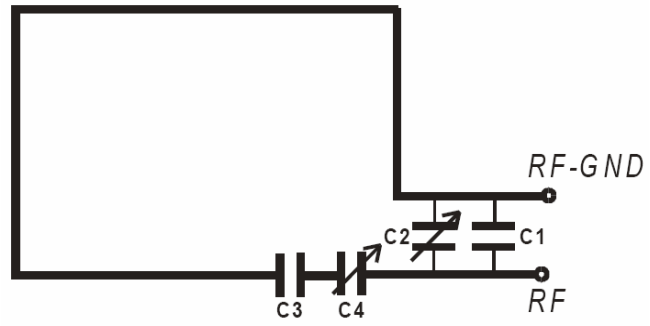

Figure 2.8. Loop antenna suggested by Radiometrix

Although the wire antenna is slightly cumbersome comparatively, this configuration was chosen because it is the simplest to build and provides the largest open ground range of 300 meters. The length of the wire should be 15.5 cm as suggested in Figure 2.9.

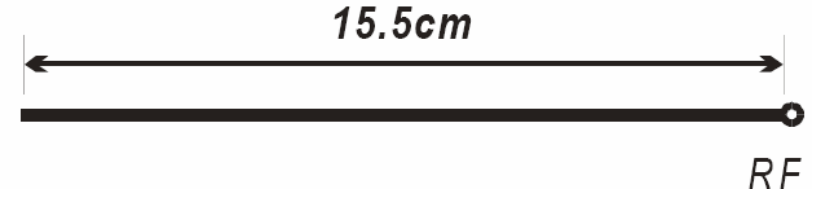

Figure 2.9. Wire antenna suggested by Radiometrix

2.3 Energy Comparison

An energy comparison between continuous and periodic transmission methods is discussed in this section. As mentioned in Chapter 1, a comparison between the methods presented by Lynch et al. (2003c) and Sazonov et al. (2004) wireless transmission is studied along with the method presented in this thesis. Table 2.1 compares the wireless transmitter's energy requirements for the previously mentioned systems with the transmitting method used by the author. This comparison is based on a monthly cycle. For the two periodic methods, once a month the system will be activated and operate for one minute. Three wireless systems are compared in this analysis. These systems are a Chipcon CC2420 radio, a Proxim RangeLAN2 7911, and a Radiometrix TX-2 transmitter. They correspond to Sazonov, Lynch, and the author's systems, respectively.

Table 2.1. Wireless energy comparison of structural health monitoring methods

Wireless System	Transmitter Power while sending data	Transmitter Power while idle	Monthly Energy Consumption
Chipcon CC2420	52 mW	0 mW	0.0031 kJ
Proxim RangeLAN2 7911	950 mW	30 mW	77.8 kJ
Radiometrix TX-2	47 mW	0 mW	0.0028 kJ

This comparison shows that continuous data transmission from a SHM system consumes more energy than periodic transmissions. In the author's method, the data being transmitted is in serial signal, "warning signal", that defines the current state of the structure. In the current configuration, a LED is connected to the receiver as seen in Figure 2.6. When this LED is illuminated no damage has occurred in the structure. Damage has been detection by the SHM system when the LED begins to blink. This method is advantages from a wireless energy consumption standpoint.

In practice, the time period between transmissions of the warning signals would be application specific. Also, this warning signal should not only imply damage has

occurred; since just as importantly the transmission of a “no damage” signal would insure proper working condition of the SHM system.

2.4 Chapter Summary

Chapter 2 presents the transmitter and receiver circuits used to meet the telemetry requirements for this project. The chapter begins by introducing the importance of wireless communication in the field of structural health monitoring and noting common approaches used in data transmission for SHM systems.

Next, the chapter focuses on the Radiometrix modules used for experiments. Details of the transmitter, receiver, and antenna that were used are discussed. Further details and specifications about the Radiometrix products can be found at www.radiometrix.com. The Radiometrix modules are good candidates for future stages of our SHM project, because of their compact size and serial communication capabilities.

Finally, the chapter compares three different methods of transmitting data from a SHM system. The comparison shows that the transmission of a warning signal at a periodic time interval is the most energy efficient method.

Chapter 3

Components of the CIMSS Structural Health Monitoring System

3.1 Introduction

The necessary components, excluding the wireless system discussed in chapter 2, that make the CSHMS functional are described in this chapter. First, PC 104 Boards, which served as the central processing unit for the CSHMS, are introduced and then the specific board, which was chosen for this application, is discussed. Next, the significance of the low cost method for impedance-based testing is discussed. Finally, an overview of power harvesting technology and its relevance to SHM applications is given. In addition to the key components that will be reviewed, an aside is also presented about digital signal processors. The significance of digital signal processors in future structural health monitoring systems will be addressed in this section.

3.2 PC/104 Boards

PC/104 Boards are actually stand alone computers that are designed for embedded applications. These boards are also commonly referred to as single board computers (SBC). This boards use a traditional microprocessor for data manipulation and mathematical calculations. PC/104 is the standard that these embedded microprocessor based boards follow. Over 100 manufactures of PC/104 boards exist on today's market. For the purpose of this research a Diamond Systems PC/104 board was chosen. This PC/104 board, referred to by Diamond Systems as Prometheus, was originally choose because of its capiblity to interface with MatLAB® and Simulink®. However, after attempting to program the necessary algorithm with Simulink®, the C++ programming

language was chosen because of the greater flexibility and control offered with C++. The key contribution of the Prometheus board is the ability to perform an FFT, which allows the programmer the ability to study the structure in the frequency domain.

The significant specifications of the Prometheus board are as follows:

- ZFx86 100 MHz CPU
- 32 MB RAM
- 16 Analog Input Channels
- 4 Analog Output Channels
- Watchdog I/O
- 24 Digital I/O Channels
- 2 MB Flash memory for system BIOS
- 32 MB Flash disk memory module (mini hard drive)

This sampling rate of the 16 analog input channels is 100 kHz divided by the number of channels being sampled. The CSHMS uses 2 analog input channel hence the maximum sampling rate is 50 kHz. ROM-DOS is used as the operating system and is loaded to the 32 MB flash disk memory module. This module provides memory storage space not only for the operating system but also the baseline measurements used for comparison in the SHM algorithm.

3.3 Integration of Low Cost Method

In order to implement the impedance-based method on the CSHMS, the low cost method for impedance measurements was used. This method provides a means for measuring impedance with the use of an expensive impedance analyzer, such as an HP 4192A analyzer. The low cost circuit use for the CSHMS is presented by Pearis *et al*. (2002). Figure 3.1 is Pearis's low cost circuit with an additional capacitor used for impedance matching. The capacity of the PZT at the mean frequency of the testing frequency range was found. This capacity was matched by C_m in Figure 3.1.

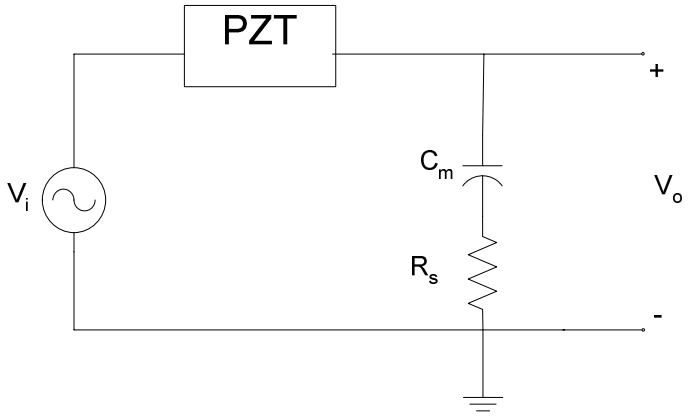

Figure 3.1. Low cost circuit with impedance matching

When R_s is small, the voltage drop across the PZT is proportional to V_o, hence the impedance across the PZT is also proportional to V_o. V_o is the voltage measured by the A/D converter.

3.4 Power Harvesting

An introduction to power harvesting is presented in the first part of this section. In the second part of this section, the importance of power harvesting in structural health monitoring applications is given.

3.4.1 Introduction

Power harvesting is a technology that recovers energy normally lost from a system to its surroundings. The research discussed in this chapter will focus on power harvesting from ambient vibrations. Piezoelectric materials are often used to convert mechanical energy in ambient vibrations to electrical energy. This scavenged electrical energy is then stored in batteries or capacitors for later use. Piezoelectric materials are capable of this conversion because they have a crystalline structure that gives this material the ability to convert a mechanical strain into an electrical current (Sodano *et al*.

2002). This is a desired material property for harvesting power from ambient vibrations. In recent years, Sodano, a researcher at CIMSS, has published many conference papers and journal articles regarding research in power harvesting. This chapter will give an overview of his work as well has some of the current requirements of today's SHM systems.

The motivation behind power harvesting technology stems from the need to replace finite energy sources, such as batteries, with devices that can generate power for the lifespan of the electronic system. An abundant array of applications of this technology currently exists. Some examples of these applications are human exercise activities such as walking or running the energy lost could be used to power a FM radio, similarly such a power harvesting device could be used to power tracking devices for wildlife applications. The applications that researchers in the SHM community are interested in involve harvesting power from ambient vibrations in a structure such as a bridge, aircraft frame, or building. This energy scavenged from ambient vibrations could be used to power a structural health monitoring device.

3.4.2 Power Harvesting in Structural Health Monitoring Systems

A major research and development issue in today's literature referring to SHM systems is the amount of power required for the system to recorded data, transmitted data, and process data, if applicable. Therefore, power supplies for SHM systems have become a key issue in this area of research. The fact that SHM systems are to be maintenance free for the lifespan of the structure, implies that the electronic components must be reliable enough to survive this lifespan and the power source must be capable of supplying power for this lifespan. The solution to meet the power requirement is to use a system that can recharge its own power source while in service.

The CSHMS currently operates at using a 5.00 Volt DC power supply and draws 1015 mA, or 5 Watts of total power when computations and transmitting are performed.

One minute is the estimated time needed to complete computations and transmission. The total energy expended for this task is 0.3 kJ.

According to the research performed by Sodano *et al*. (2004), a battery with a capacity of 1000 mAh can be charged to 1.2 Volts in 32 hours. Assuming a battery with a capacity of 1000 mAh at 1.0 Volts exhibits a similar charging time, then five 1.0 Volt batteries in a series configuration could be used to supply the needed voltage and current to operate the CSHMS. The significance of his research in our application is that a timeline can be established regarding how often testing of the structure can be performed. In this case, Sodano's research shows that testing of the structure can be performed every 32 hours. However, since ambient vibrations vary greatly from structure to structure charging time will be application specific. The use of vibration absorbers, which would contain the PZTs needed to harvest energy, may aid in the harvesting process. The proposed power harvesting circuit for the CSHMS is depicted in Figure 3.2. This configuration would meet the power requirements of the CSHMS.

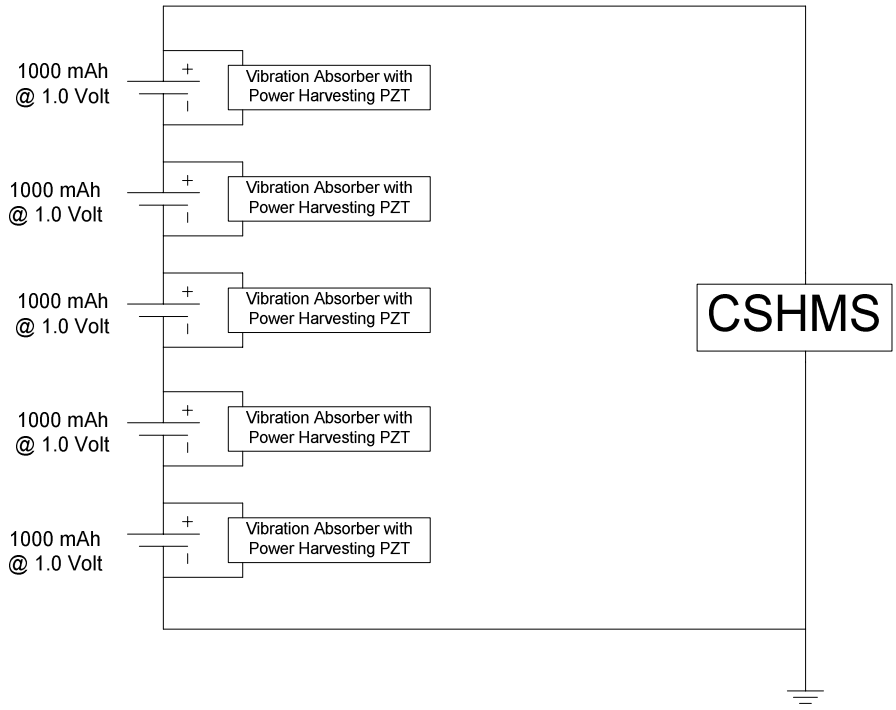

Figure 3.2. Power harvesting circuit for CSHMS

In Figure 3.2, five batteries are shown in a series configuration. This configuration allows for the required voltage and current of the CSHMS to be meet. Shown in parallel with each battery is a PZT mounted to a vibration absorber. This vibration absorber would be mounted to the structure in the proximity of the CSHMS and would harvest the energy needed to recharge each battery.

3.5 Digital Signal Processors

Digital Signal Processors (DSP) are a subset of microprocessors that are designed specifically for mathematical calculations (Smith 1999). In general, microprocessors have been developed to perform two tasks: data manipulation and mathematical calculations. Designing a microprocessor to perform both tasks efficiently can become expensive. Typically, microprocessors that are found in personal computers, such has a Pentium® type processor, are specifically designed for data manipulations. Since DSPs are specifically designed to perform mathematical operations, they are ideal candidates for data acquisition and processing applications. The major advantage of DSPs is that execution time of a program is limited almost entirely by the number of mathematical calculations to be performed, i.e. the number of multiplications and additions. This attribute give DSPs a clear advantage over traditional microprocessors.

DSPs are generally purchased in three packages: the core, the processor, or the board. The core refers to the part of the processor that includes data registers, multipliers, the ALU, the address generator, and program sequencer (Smith 1999). The processor refers to the core plus memory and a way to interface with other devices. The board refers to the processor plus additional memory, EPROM interfaces, A/D and/or D/A converters. Generally, DSP boards are produced by third party developers. The basic components of a DSP boards used for data acquisition and processing are listed and discussed in this section. Such boards have direct applications to future structural health monitoring systems.

A parallel or serial port is needed on the board to establish a means to communicate with a host computer. In the future, the use of USB ports or wireless communication may become a common practice.

A DC power supply of 1.8 V, 3.3 V, or 5 V is a standard necessity to run the DSP chip and peripherals.

Analog to digital (A/D) are needed for data acquisition. The two common configurations for A/D converters are a scanning or multiplexing configuration. In general, the scanning configuration would utilize one A/D for all A/D channels. The effective sampling rate would then be the maximum sampling rate of the A/D divided by the number of A/D channels being used. For example, if an A/D had a maximum sampling rate of 250 kHz and four channels were scanned using this A/D the maximum sampling rate that could be achieved per channel would be 62.5 kHz. For a multiplexing configuration, all four channels could be sampled at 250 kHz. However, the most effective way to sample multiple channels while maintaining a high sampling rate is to use an A/D converter for each channel. Using multiple A/D converters is will ensure that the data acquisition system will be capable of high sampling rates.

3.6 Chapter Summary

This chapter introduces the key components that were needed to make the CSHMS functional. The ability to measure impedance without the use of an impedance analyzer was one of the first tasks conquered by Pearis (2002). The addition of a microprocessor board to capture this impedance signal and run the FFT algorithm needed to analysis this impedance data was presented in this chapter. In addition, a power harvesting circuit is proposed based on the research of Sodano (2004). This circuit would allow the CSHMS to function indefinitely, in a practical application.

Chapter 4

Techniques to Detect Damage in Structures

4.1 Introduction

Detecting the existence of damage is the first level of the classification system mentioned in chapter 1 that was devised by Rytter (1993) and later revised by Inman (2003). Damage detection was the primary goal of the research presented here and served as the first step in the development of the CSHMS.

Two damage detection techniques were considered for our prototype patch. The first technique was the impedance based approach and the other technique was based on shifts in the Frequency Response Function (FRF). The prototype CIMSS Structural Health Monitoring System (CSHMS) has successfully used each technique. The following section will present impedance testing of a composite plate and resonant frequency shifts in FRF. Both of these test were carried out on the CSHMS develop. Also, presented will be a resonant frequency test using dSPACE for data acquisition and impedance testing of an aircraft rib using the HP 4192A impedance analyzer.

For the proof of concept CSHMS, using resonant frequency shifts in place of the impedance method is far less expensive because the sampling rate can be reduced, therefore cheaper data acquisition boards can be used. The desired frequency for the impedance method is generally considered greater than 30 kHz (Park *et al.* 2003), therefore the sampling rate would need to be 300 kHz since the standard practice in digital signal processing is to sample at ten times the desired frequency to be measured. For the resonant frequency shift method, the desired frequency for the experiments conducted was 5 kHz, implying that the sampling rate would need to be 50 kHz. The lower sampling rate for the resonant frequency shift method qualifies this method as a

good candidate for a prototype SHM system. A successful impedance test was conducted using the CSHMS. Although the data obtained from this test was noisy the damage metric computed from the data successfully detected the damage introduced to the composite plate.

4.2 Impedance

Impedance Based Structural Health Monitoring applied to a Composite Plate

A goal of this research was to test a composite plate using an impedance-based algorithm that would be executed on the developed CSHMS. The low cost method, implemented by Peairs (2002), is necessary when using an impedance-based technique coupled with the CSHMS developed.

Figure 4.1 shows the experimental setup of the composite plate that was tested. The boundary conditions for this experiment were free-free and the input swept sine wave ranged from 8 kHz to 12.5 kHz. As can be seen in Figure 4.1, one PZT was mounted on the composite plate and served as the actuator and sensor since the low cost method was utilized.

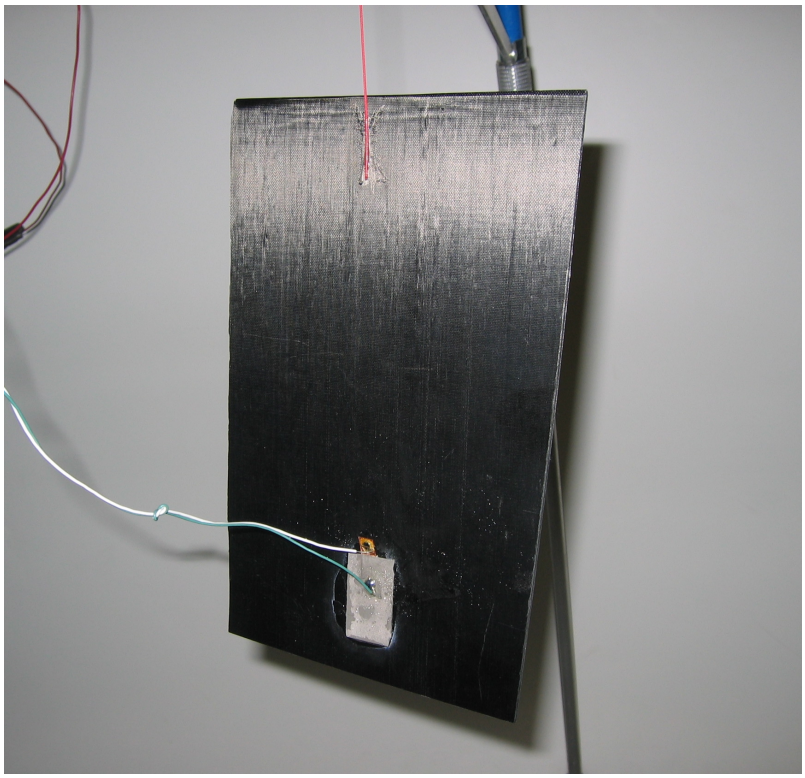

Figure 4.1. Experimental setup of composite plate

Damage was introduce to the composite plate by using a flat head screw driver and hammer. The resulting 3/8" by 1/8" gouge in the composite plate is shown in Figure 4.2. Other discontinuities in the composite plate, in Figure 4.2, to the right and below the gouge existed before and after the creation of the gouge. These discontinuities have no influence on the detection algorithm since they existed during the recording of the baseline data set.

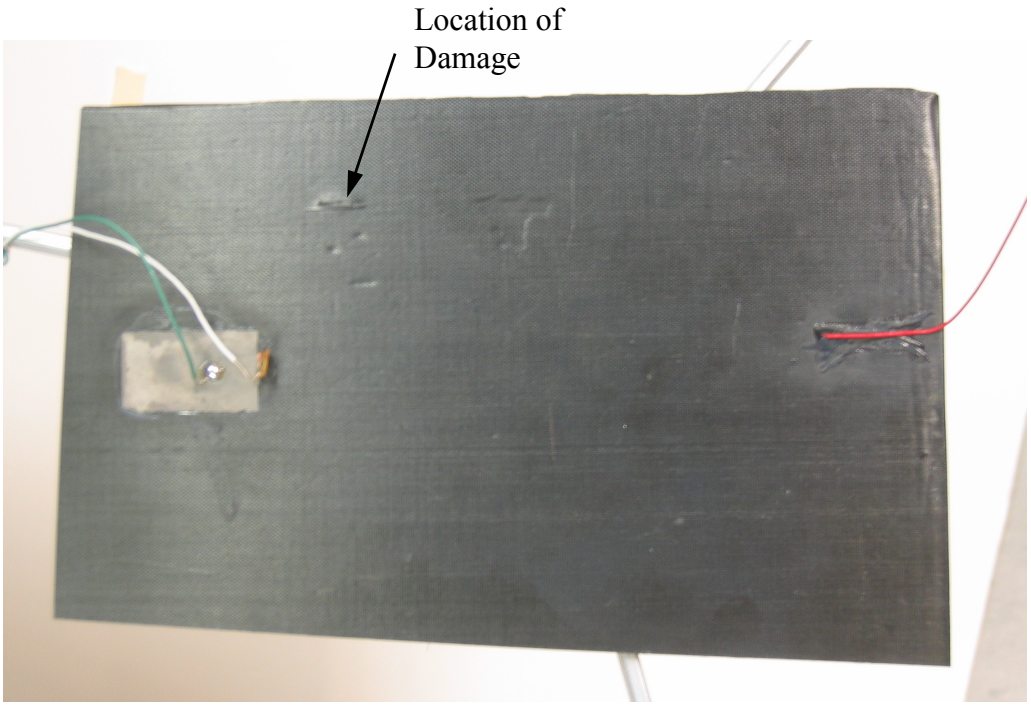

Figure 4.2. Composite plate with damage

Results from impedance testing are often shown by the real part of the impedance signal. These plots can serve as a qualitative approach for damage identification (Park 2003). A scalar damage metric is traditionally used to quantify damage. Past researchers (Sun 1995) used a statistical algorithm based on a frequency-by-frequency comparison, which is referred to as the damage metric. The equation for the damage metric is shown in equation 4.1,

$$M = \sum_{i=1}^{n} \sqrt{\frac{(\mathrm{Re}(Z_{i,1}) - \mathrm{Re}(Z_{i,2}))^2}{(\mathrm{Re}(Z_{i,1}))^2}} \qquad \text{- (4.1)}$$

M is the damage metric, $Z_{i,1}$ is the impedance of PZT measured at healthy conditions (baseline measurement), and $Z_{i,2}$ is the impedance for the comparison to the healthy conditions at frequency interval i. Generally stated, the greater the numerical value of the damage metric the larger the difference between the healthy condition and the tested condition indicating damage has occurred within the structure being tested. In equation

4.1, only the real part of the impedance signal is of interest when computing the damage metric.

The damage metric defined above was utilized in experimental test of the composite plate. Figure 4.3 shows the real part of the impedance signal obtained from testing of the composite plate. The impedance signal obtained from the experiment did not contain sharp peaks because of three reasons. First, composites have significantly higher damping characteristics, implying that the response signal will not be as large in magnitude as for a metallic material. Secondly, due to digital signal processing issues the input sweep-sine excitation interval was very short, therefore the excitation of the structure was small and this resulted in a small response. Using the CSHMS, a sweep sine wave excited the structure for 100 msec over a frequency range of 8 kHz to 12.5 kHz. However, after qualitative analysis of the impedance signal the range of 11.5 kHz to 12.3 kHz showed significant changes in the real part of the impedance signal. The damage metric computed for this range shows that the test was sensitive to the gouge introduced on the composite plate.

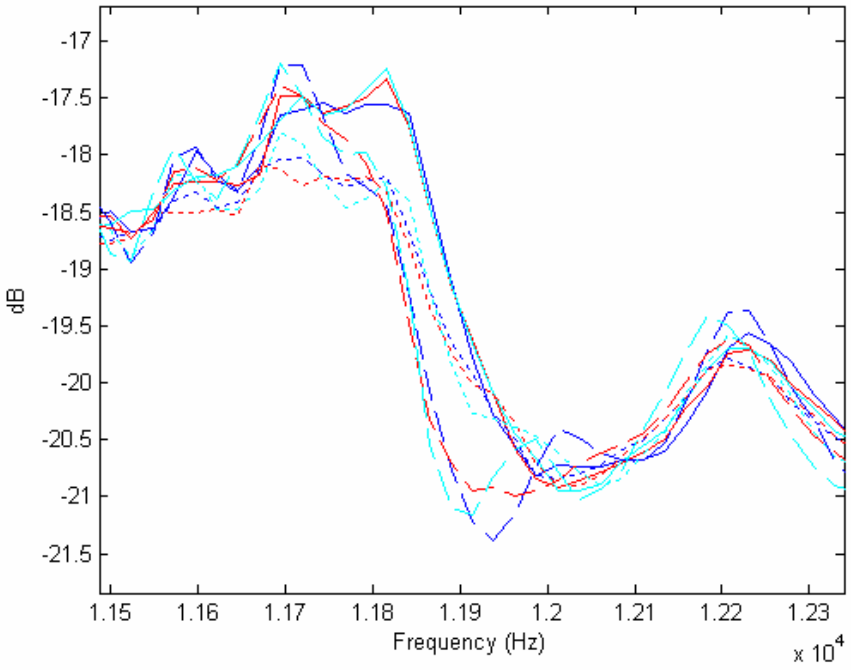

Figure 4.3. Composite plate data recorded with the CSHMS

The plot shown in Figure 4.3 does contain noise since our resolution with the CSHMS is less than desired. Therefore, the results were checked using the HP 4192A impedance analyzer. The HP 4192A divides the desired frequency range into 400 segments, then steps through this frequency range one segment at a time recording four averages at each frequency. The algorithm for the impedance analyzer is significantly different from the impedance algorithm programmed on the CSHMS.

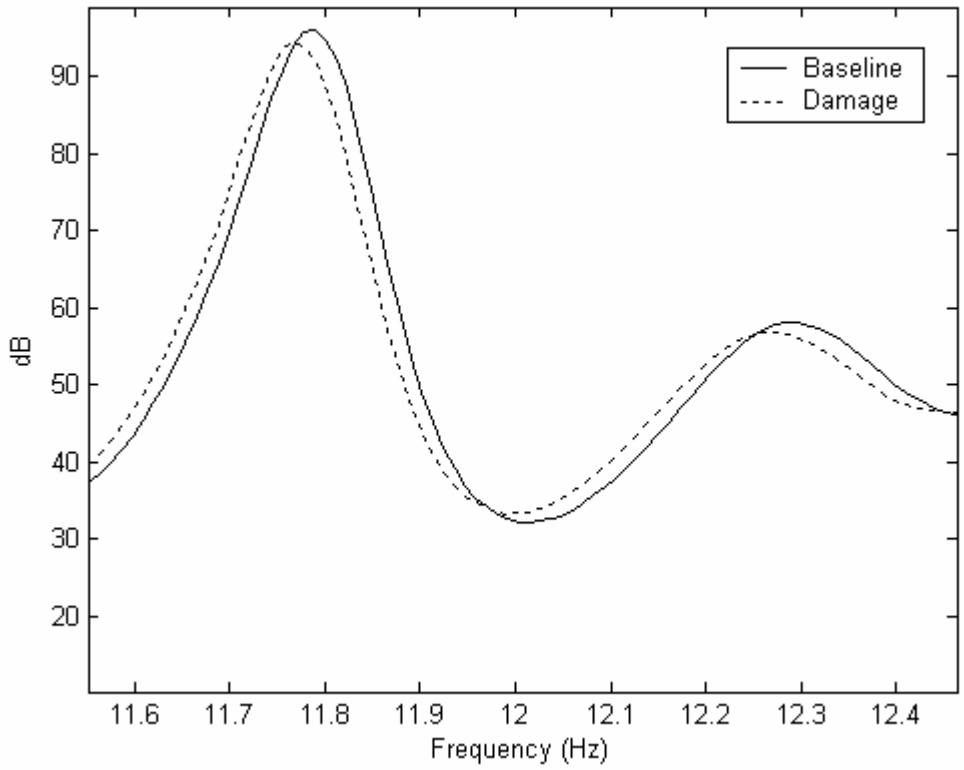

Figure 4.4. Composite plate data recorded with the HP 4192A Impedance Analyzer

The damage metrics for the 9 data sets are shown in Figure 4.5. The first baseline data set can be considered data set zero and was used as the baseline for all future comparisons. Hence, Figure 4.5 shows the comparisons of sequential data sets against the data set zero, hence only 8 damage metrics need to be computed. Sets 1 and 2 are baseline data sets. Sets 3, 4, and 5 are after the initial Level 1 damage was introduced to the composite plate. Sets 6, 7, and 8 are after additional damage was introduced to the composite plate, i.e. Level 2 damage. The damage metric values in Figure 4.5 show that threshold values could be set for each damage scenario.

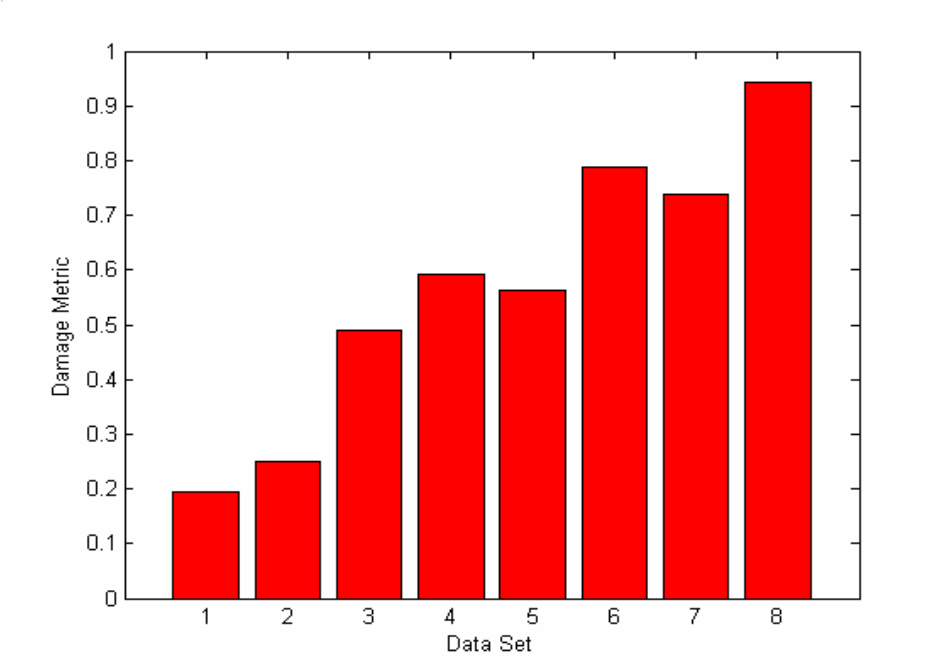

Figure 4.5. Damage metric values from composite plate experiment

Figure 4.6 represents the average damage metric for each of the three damage cases which are the baseline case, level 1 damage case, and level 2 damage case.

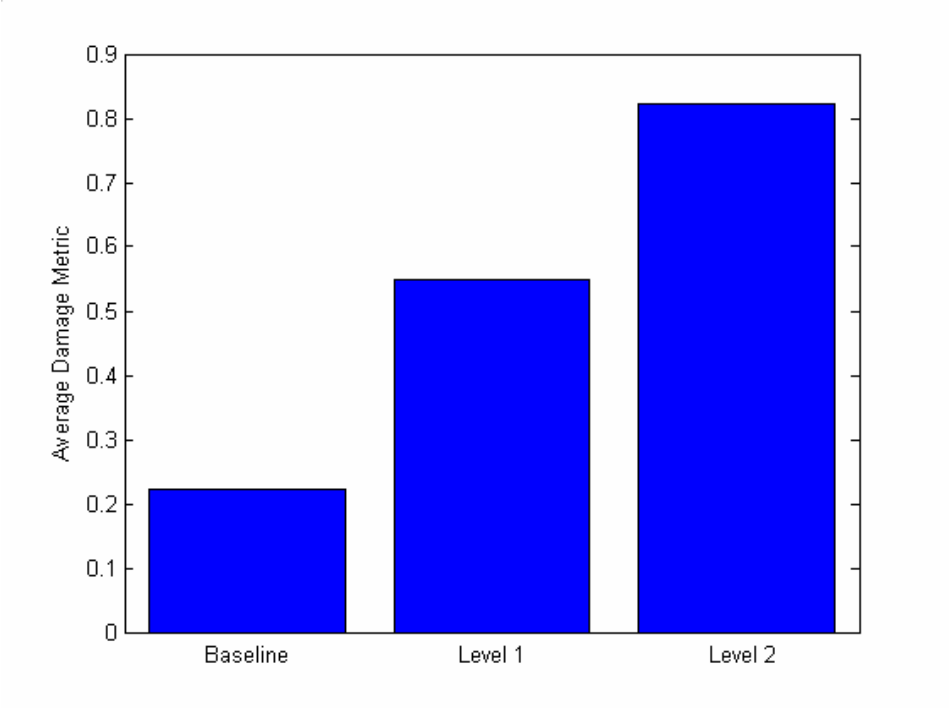

Figure 4.6. Average damage metric values from composite plate experiment

The result of this composite beam experiment demonstrates that the CSHMS developed is capable of detecting minute damage within a composite plate. In practice, the CSHMS is capable of detecting damage when a predetermined threshold is exceeded.

Impedance Testing of an Aircraft Rib

In order to demonstrate the practical use of the impedance method and the CSHMS developed, testing was performed on an aircraft rib supplied by the United States Air Force. This rib is shown in Figure 4.7. All data was recorded using the HP 4192A impedance analyzer, since high frequency testing was desired. In addition to the high frequency testing, one set of data from 8 kHz to 13 kHz was recorded to show that damage detection was possible in this range. Using the CSHMS, successful results were obtained in this frequency range during the composite plate experiment. The structure shown in Figure 4.7 suffers from habitual fatigue failures. Figure 4.8 shows the location of the sensing/actuating PZT.

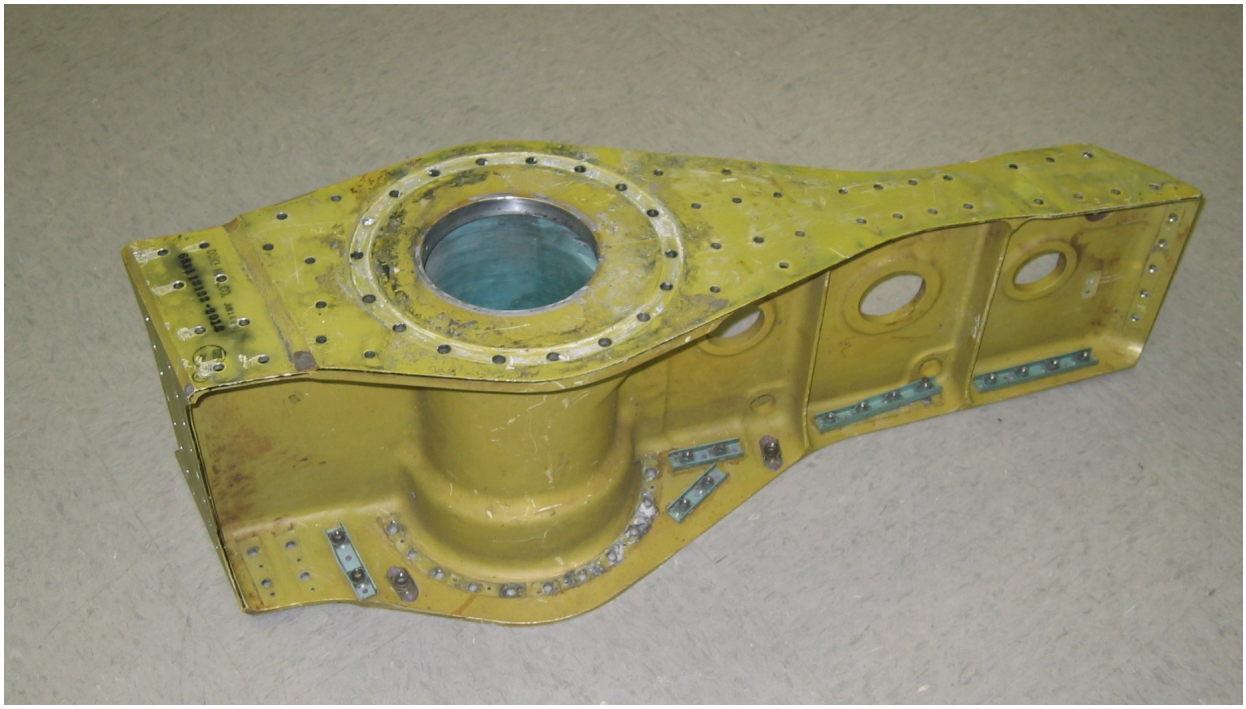

Figure 4.7. Aircraft rib supplied by United States Air Force

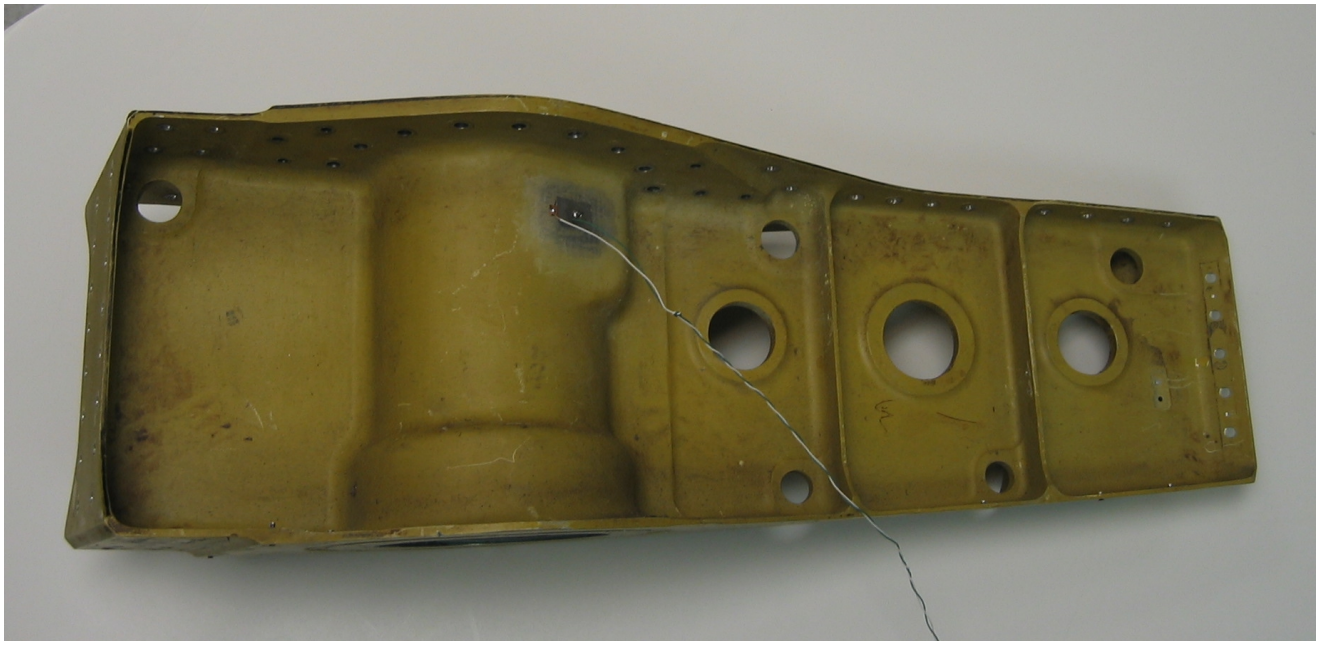

Figure 4.8. Aircraft rib with sensing/actuating PZT mounted

Figure 4.9 shows the location were the fatigue cracks initiate in this structure. The fatigue crack initiates along a fillet in an area were the inner radius changes. The "white" section of Figure 4.10 represents the area where the fatigue crack propagated.

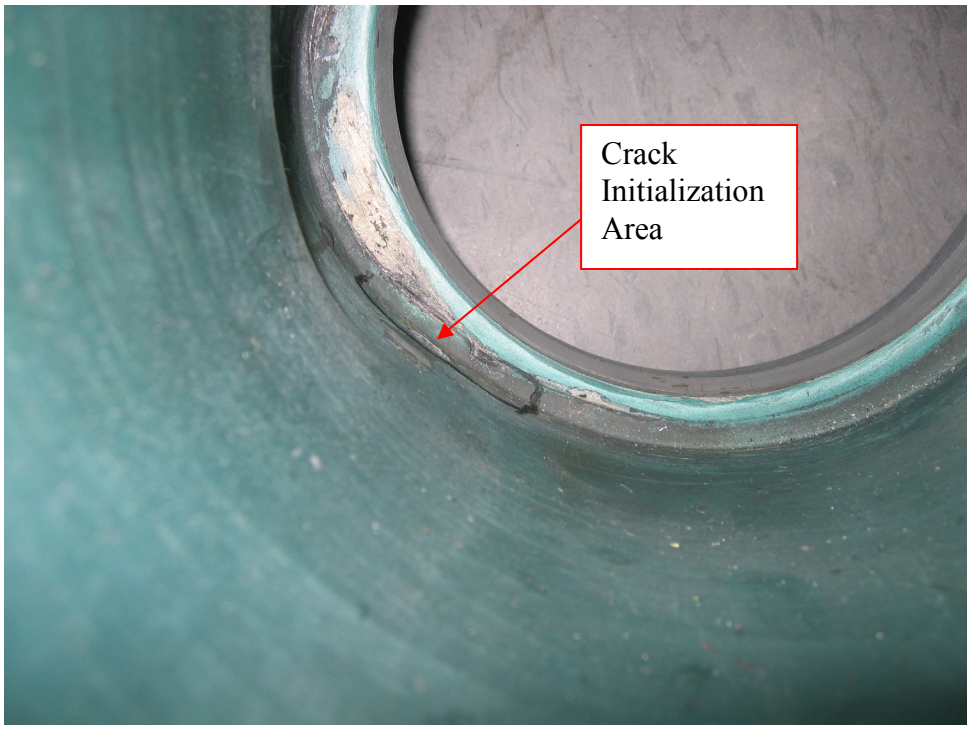

Figure 4.9. Fatigue crack initialization area

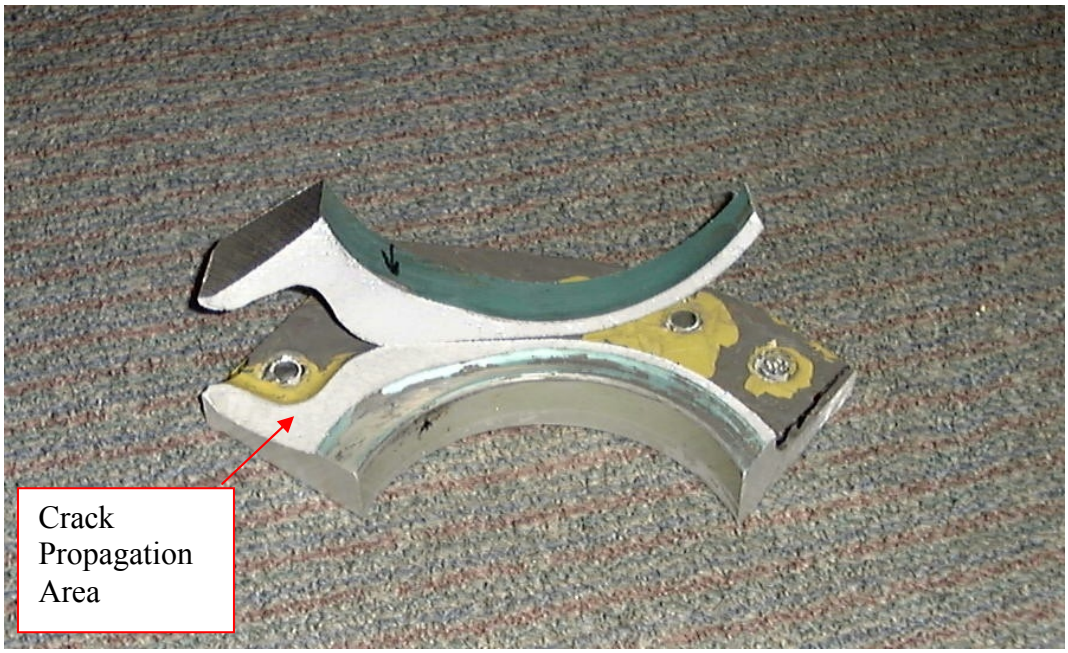

Figure 4.10. Section of aircraft rib that failed from fatigue

The procedure for testing the aircraft rib followed the standard pattern: baseline measurements of the structure were recorded, the structure was subjected to damage and

the first damage measurements were recorded, additional damage was introduced and the second damage measurements were recorded. The HP 4192A impedance analyzer was used to test over three frequency ranges. High frequency testing is the major reason the impedance analyzer was used to conduct this test. The SHM system developed should only be used to record excitation frequencies up to 13 kHz. In pervious experiments with the composite plate, testing was successfully performed in the 8 kHz to 12.5 kHz range. Therefore, the first frequency range for testing was 8 kHz to 13 kHz. Two addition data sets of 50 kHz to 60 kHz and 150 kHz to 160 kHz were also chosen. In aircraft applications, high frequency testing is desired because lower frequency testing could be corrupted by ambient mechanical vibrations.

Figure 4.9 is a picture of the fatigue crack initiation area before damage was introduced. For each frequency range five data sets were recorded. Three of the data sets represent the baseline case. For the Damage 1 case, a flat-head screw driver and hammer were used to create a notch in the fatigue crack initiation area. For the Damage 2 case, a Dremel® tool was used to introduce additional damage in the fatigue crack initiation area. Figure 4.11 is a picture of the fatigue crack initial area after damage is introduced with the Dremel® tool.

Figure 4.11. Damage introduced to structure

Figure 4.12 shows only a portion of the entire 8 kHz to 13 kHz frequency range tested so that features of the impedance measurement can be visually appreciated. Qualitatively, the three baseline measurements are almost one in the same and the two damage cases tend to deviate from the baseline cases as expected. However, the two damage cases do not vary between themselves as much as expected.

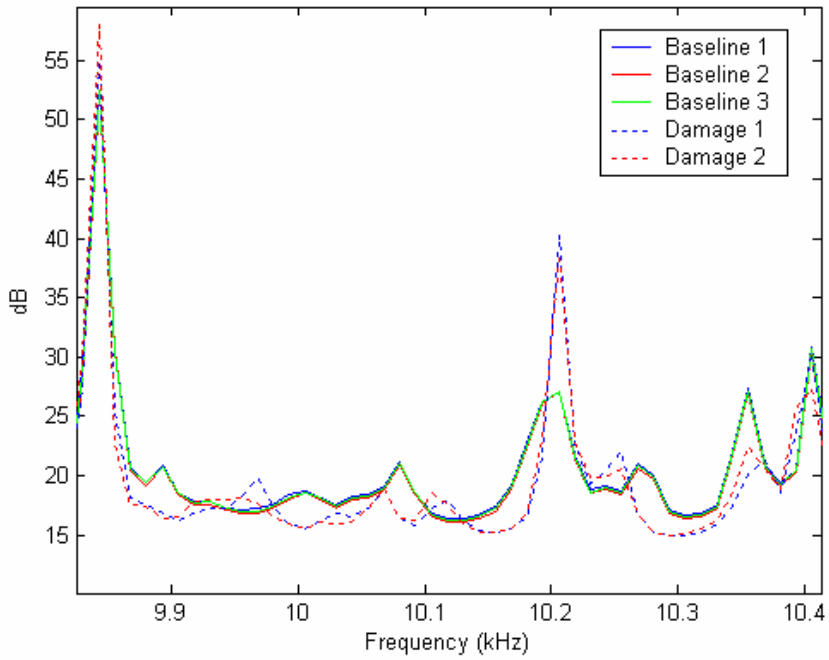

Figure 4.12. Plot of real part of impedance for 8 kHz to 13 kHz test range

In order to quantitatively compare the impedance signals within this frequency range, the damage metric analysis is applied to the impedance data sets. The result of this analysis is shown in Figure 4.13. The first baseline data set is assumed to be data set zero, then data sets 1, 2, 3, and 4 are compared to data set zero. Data sets 1 and 2 are the other two baseline cases. Data sets 3 and 4 are damage cases 1 and 2, respectively. The damage metric was calculated across the entire test range of 8 kHz to 13 kHz. The results from this frequency range appear to indicate that the test is sensitive to damage but not sensitive to the degree of damage. This is a shortcoming of low frequency testing. The damage metric values computed are 0.3225, 0.1511, 2.0804, and 2.0380 for data sets 1, 2, 3, and 4, respectively.

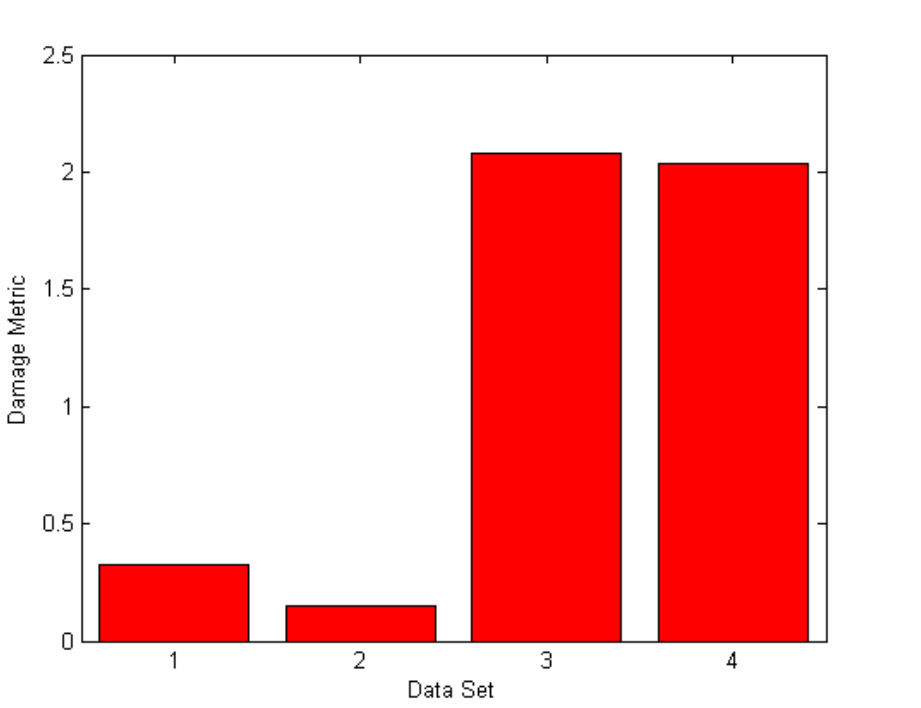

Figure 4.13. Damage metric for the 8 kHz to 13 kHz case

The same type of analysis conducted for the 8 kHz to 13 kHz range was repeated for the other two frequency ranges.

Figure 4.14 is a portion of the 50 kHz to 60 kHz frequency range tested. Figure 4.15 is the result of the damage metric analysis across the 50 kHz to 60 kHz range. The result of the damage metric analysis shows that this frequency range is sensitive to the amount of damage since the damage 1 case is represented by data set 3 and the damage 2 case is represented by data set 4. The damage metric values computed are 0.2077, 0.3217, 2.3489, and 5.7675 for data sets 1, 2, 3, and 4, respectively.

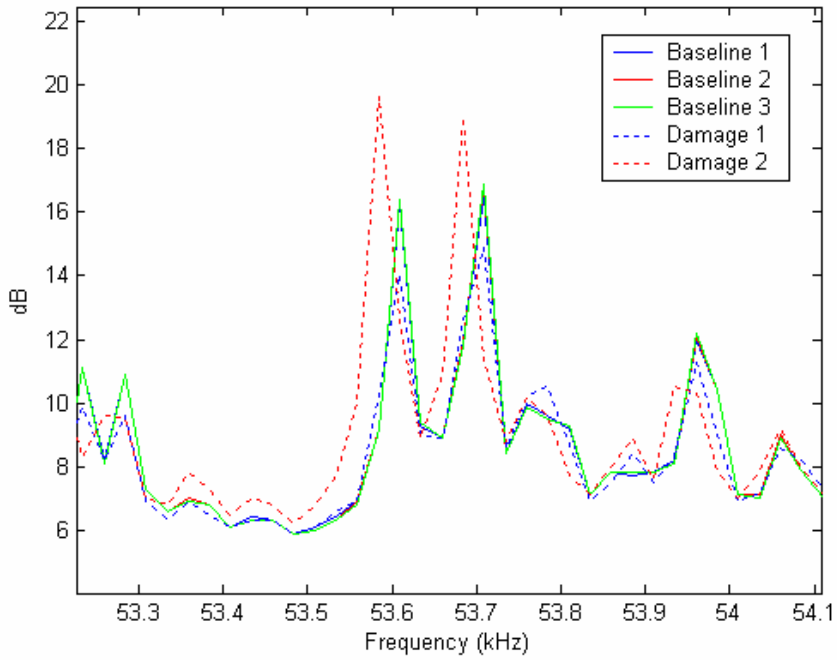

Figure 4.14. Plot of real part on impedance for 50 kHz to 60 kHz test range

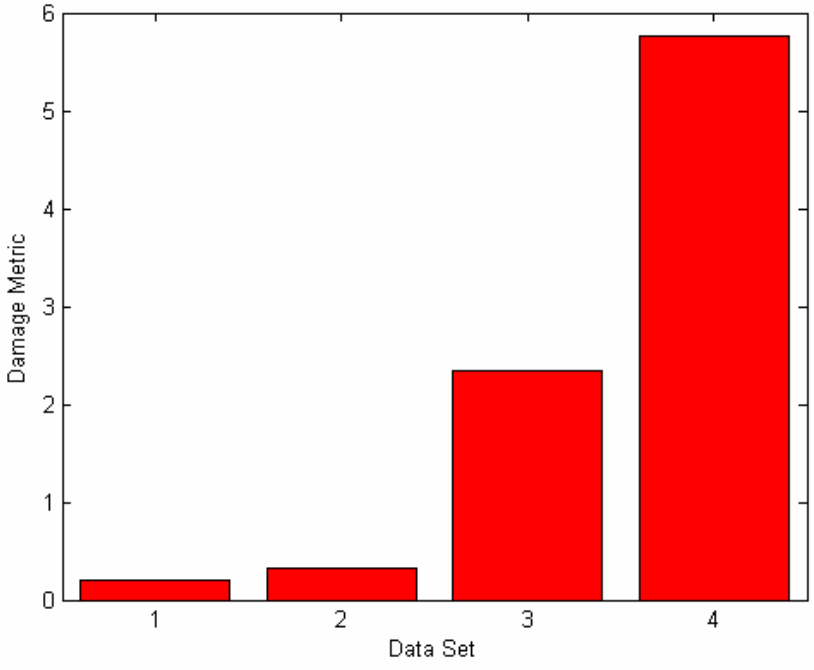

Figure 4.15. Damage metric for the 50 kHz to 60 kHz case

Figure 4.16 is a portion of the 150 kHz to 160 kHz frequency range tested. Figure 4.17 is the result of the damage metric analysis across the 150 kHz to 160 kHz range. The result of the damage metric analysis shows that this frequency range is sensitive to the amount of damage, since the damage 1 case is represented by data set 3 and the damage 2 case is represented by data set 4. The damage metric values computed are 0.0683, 0.0416, 0.9595, and 2.1977 for data sets 1, 2, 3, and 4, respectively.

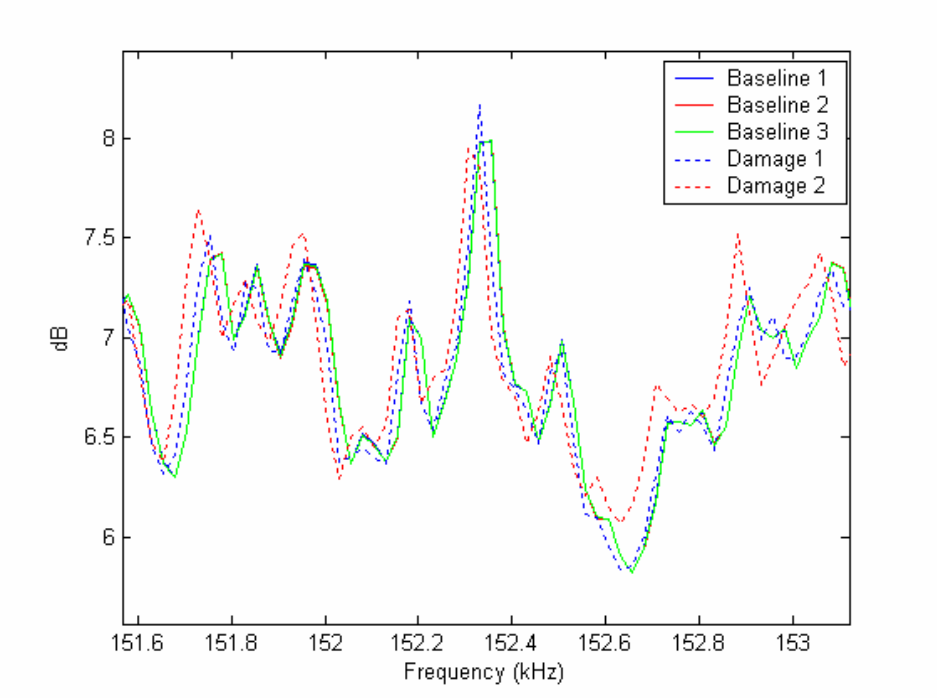

Figure 4.16. Plot of real part on impedance for 150 kHz to 160 kHz test range

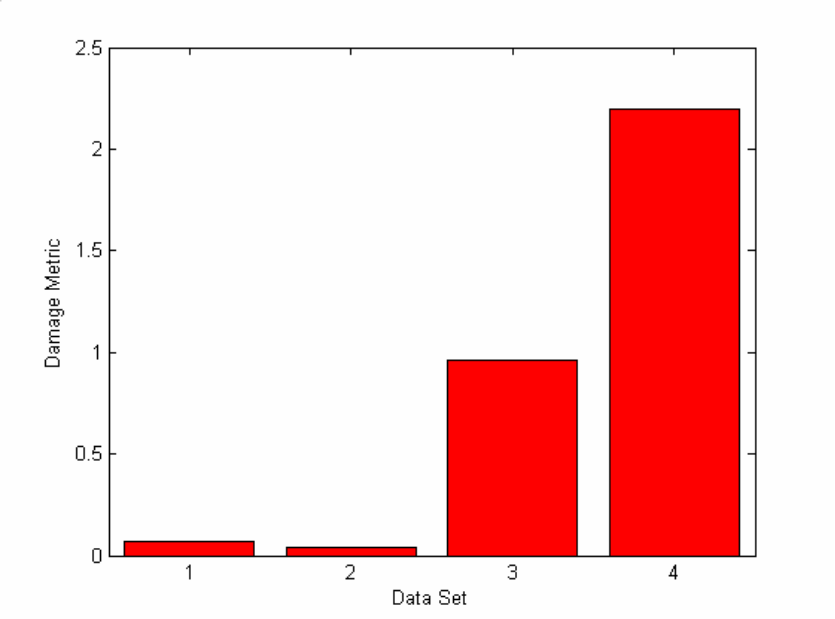

Figure 4.17. Damage metric for the 150 kHz to 160 kHz case

The results of the aircraft rib test show that low frequency testing maybe able to detect damage not the degree of damage, hence high frequency testing is desired CSHMS. The prototype CSHMS developed can record response data up to about 13 kHz with acceptable resolution. However, the next phase of research should focus on increasing the sampling rate of the CSHMS so that the higher frequency ranges can be used to obtain more detailed damage information.

4.3 Resonant Frequency Shifts

Resonant Frequency Shifts in Frequency Response Functions

This technique used is based on fundamental vibration theory. The concept is based on:

$$\omega_n = \sqrt{\frac{k}{m}} \qquad \text{- (4.2)}$$

where ω_n is natural frequency, k is stiffness, and m is mass. Assuming m is constant in equation 4.2, than a reduction in ω_n would indicate a decrease in k. In SHM, a reduction in k is generally considered damage to a structure. Therefore, being able to detect a decrease in ω_n is analogous to detecting damage within a structure. Hence, as the stiffness of a structure deteriorates due to damage, the natural frequencies within that structure will decrease. However, the addition and subtraction of stiffness to a structure is not a simple task. Therefore, for experimental purposes the mathematical relationship in equation 4.2 will be used to understand the concept that an increase in mass to a structure will result in a decrease in ω_n.

To summarize, for experimental purposes the mass (m) will be changed instead of the stiffness (k). In practice, the mass will remain constant, therefore changes detected in ω_n will be assumed to be changes in stiffness, i.e. damage in the structure.

Figures 4.18 and 4.19 are pictures of a 1/8" by 2" by 24" aluminum cantilever beam with six holes drilled uniformly along the beam. In the holes, cap head bolts and nuts are added to the beam to simulate damage based on the previously stated concept. One cap head bolt and nut is assumed to be one mass and each mass is 2.8 grams (0.10 ounces). The holes drilled in the beam for the addition of mass are labeled 1 through 6 from left to right in Figures 4.18 and 4.19. These mass locations are also labeled in the beam schematic shown in Figure 4.20.

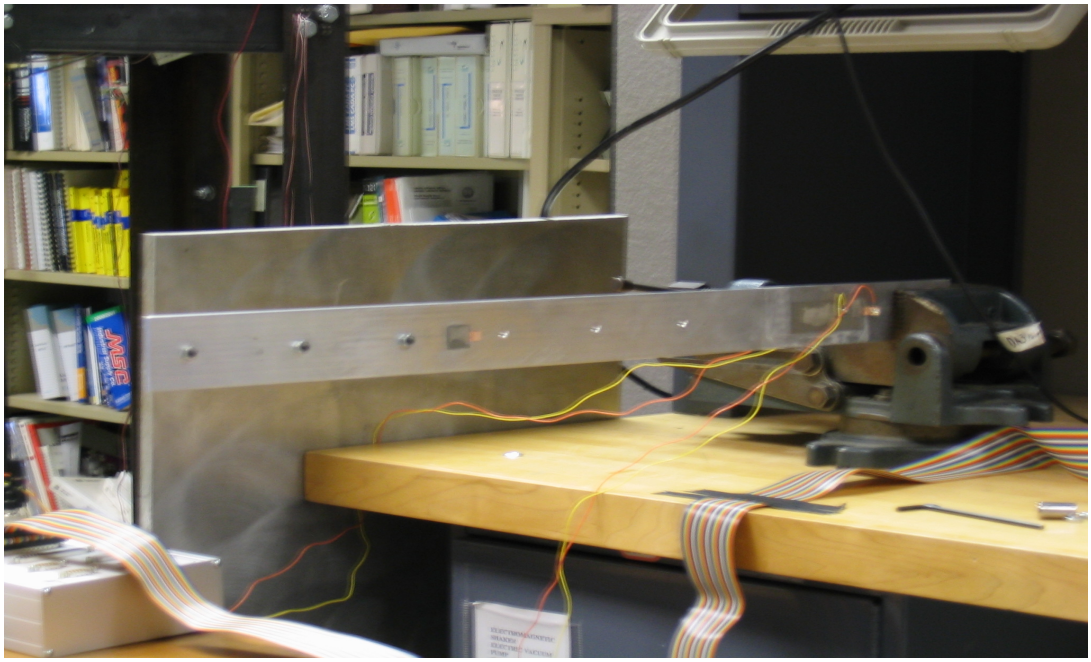

Figure 4.18. Experimental setup of six hole aluminum beam

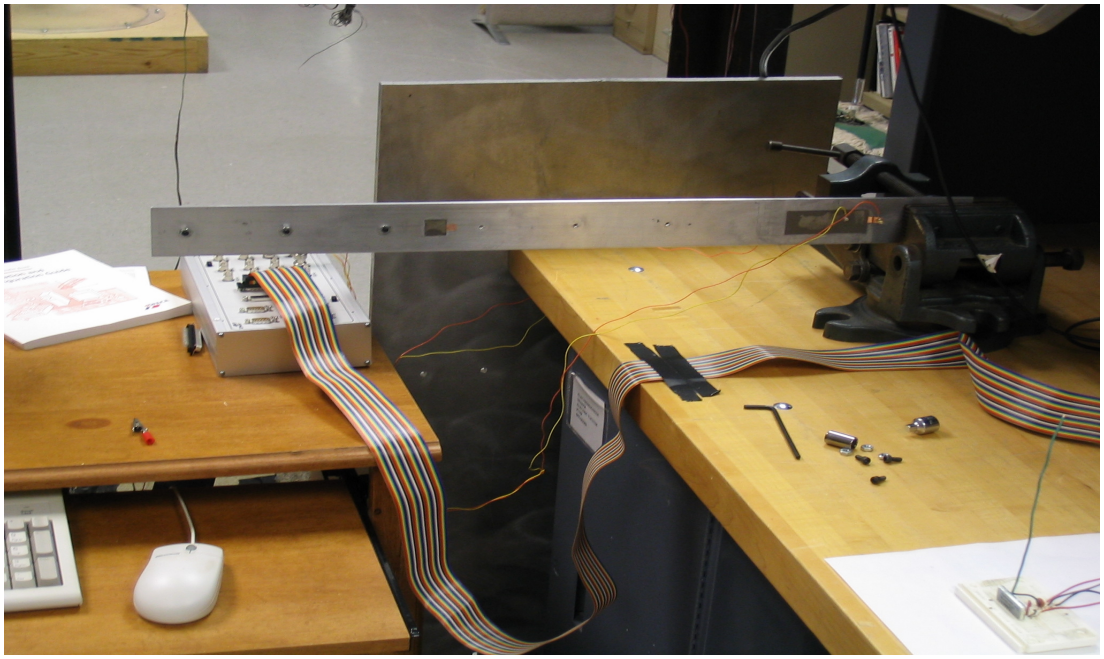

Figure 4.19. Experimental setup of six hole aluminum beam

Figure 4.20 is a schematic of the aluminum beam pictured in Figures 4.18 and 4.19. Figure 4.20 shows the dimensions of the cantilever beam and how the mass locations are labeled.

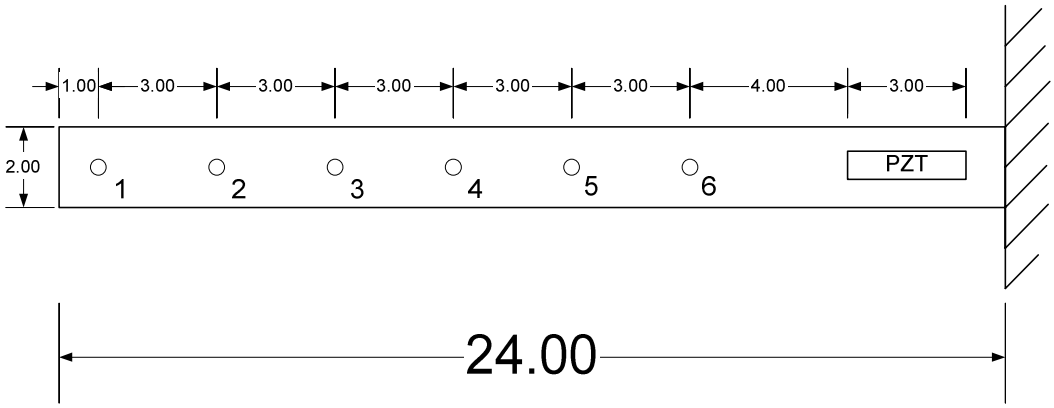

Figure 4.20. Schematic of six hole aluminum beam

Results from dSPACE

A dSPACE ds1104 control board was used as the data acquisition tool before the PC 104 board was successfully programmed and implemented as the CSHMS. This very expensive control board is capable of 16 bit analog to digital sampling rates of 500 kHz. For 12 bit data the control board is capable of analog to digital sampling rates of 1.25 MHz. This ds1104 control board is intended to be used as a rapid prototyping system for digital signal processors.

The results in this section were preliminary results that were obtained to test the resonant frequency shift concept. Qualitative analysis of the following frequency response functions show that some changes have occurred to the structural system. These frequency response functions are shown in Figure 4.21, 4.22, and 4.23. However, qualitative observation is not enough to determine if sufficient damage has occurred in a

structural system. Therefore, two quantitative techniques are used to access the state of damage within the beam. The two quantifying techniques are the damage metric and damage index. The damage metric was introduced in the composite plate section. The damage index will be introduced in the following paragraph and is the bases of the resonant frequency shift method.

The damage index technique was alluded to earlier and uses shifts in resonant frequency or peaks of the FRF to estimate if damage has occurred and the amount of relative damage that has occurred. For this technique damage is quantified by a damage index DI_n shown in equation 4.3:

$$DI_n = 1 - \frac{freq_{test}}{freq_{baseline}} \qquad \text{- (4.3)}$$

where DI_n is the damage index at some peak of interest n, $freq_{test}$ is the frequency of the peak at any test time after the baseline, and $freq_{baseline}$ is the frequency of the peak when the initial baseline was obtained.

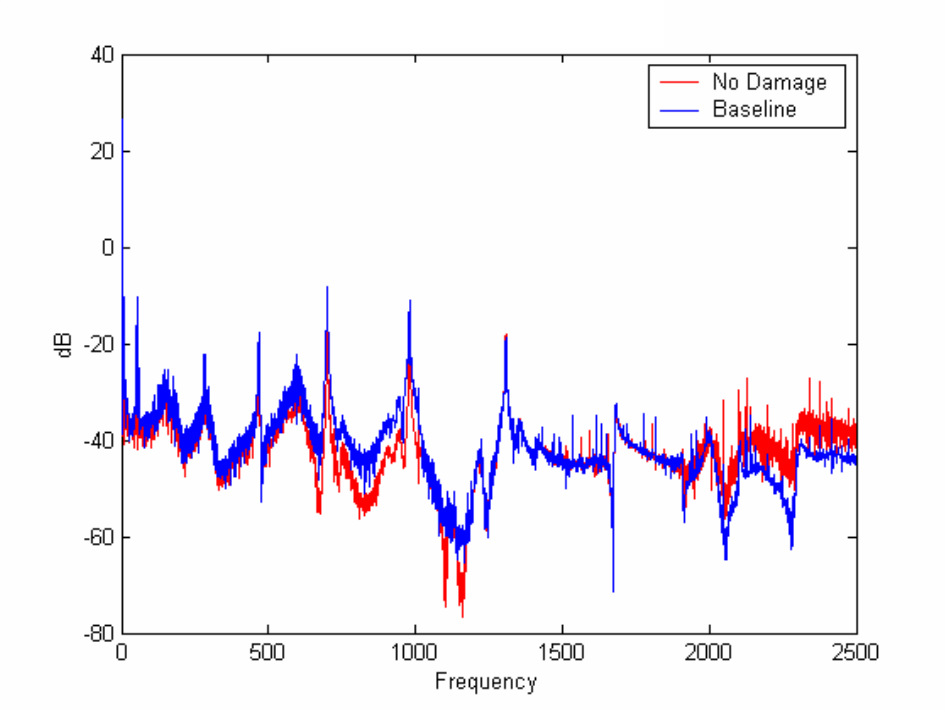

Figure 4.21. FRF when no damage is introduced

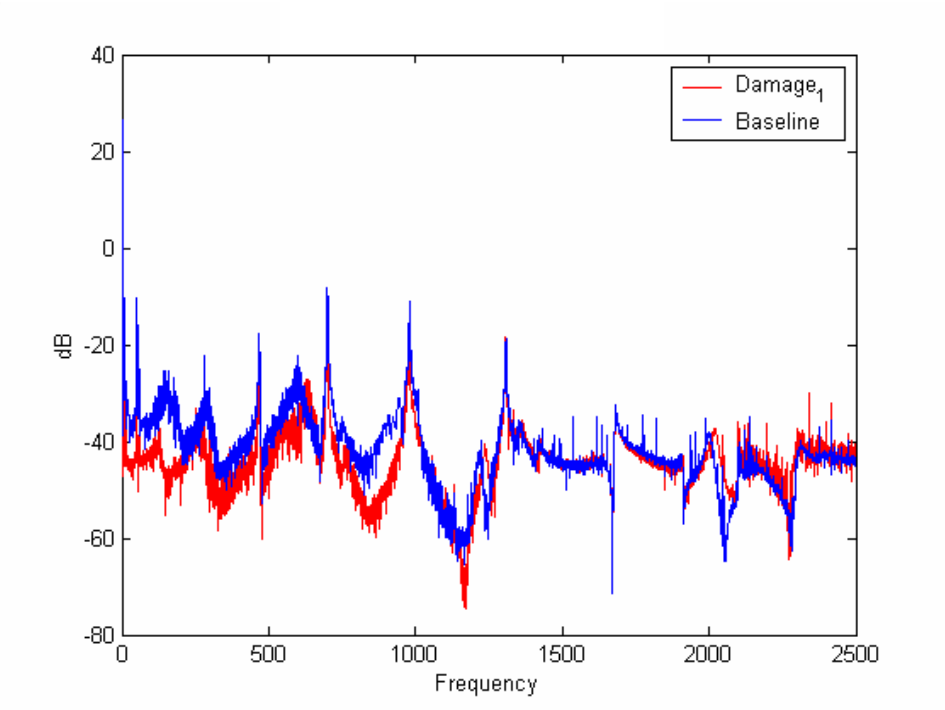

Figure 4.22. FRF when one mass is introduced at location 1

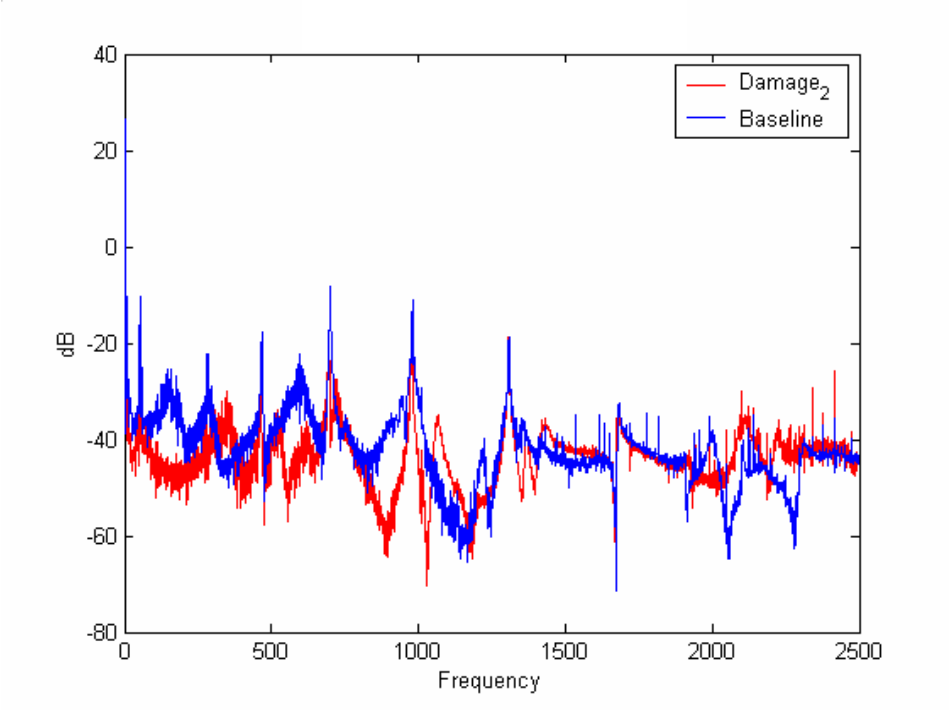

Figure 4.23. FRF when two masses are introduced at locations 1 and 2

Figure 4.24 compares three different damage cases. Data sets 1, 2, 3, and 4 were recorded when no damage was introduced to the system and are the baseline data sets for this experiment. A slight change in boundary conditions occurred between data sets 1, 2, 3, and 4 and the initial baseline frequency. This change in boundary conditions explains the negative damage index values for the four baseline data sets. Data sets 5, 6, 7, 8, and 9 were taken when one mass was added at location 1 and data sets 10, 11, 12 were recorded when two masses were added at locations 1 and 2. For each of these damage cases five data sets were recorded; however, because of a lack of repeatability, which will be discussed at the end of this section, one of the baseline data sets and two of the Damage 2 data sets were omitted.

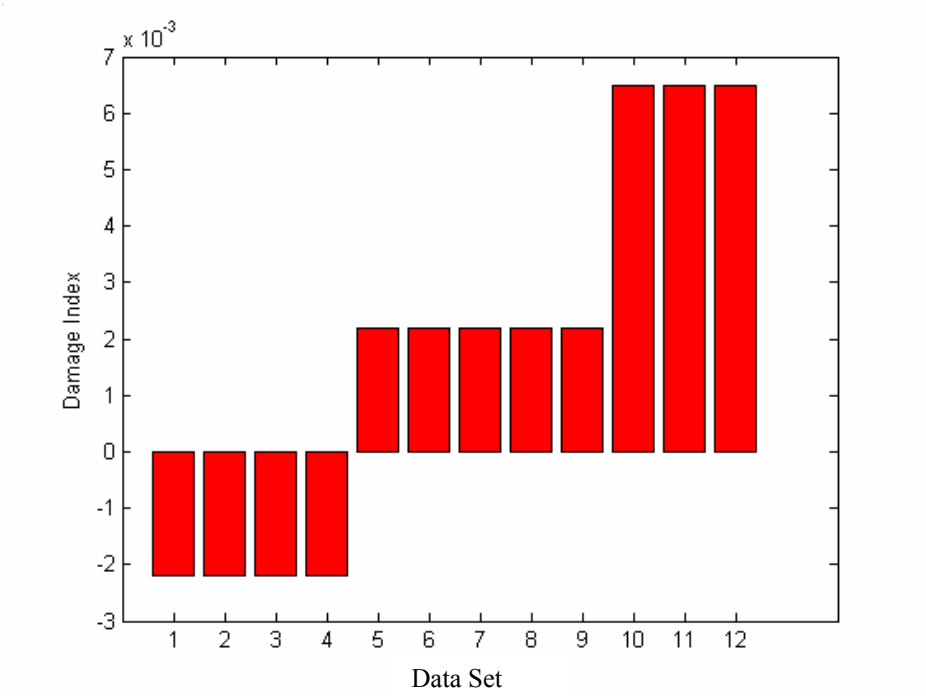

Figure 4.24. Damage index values for three different damage cases

The next technique uses the damage metric method, discussed in the composite plate section, to quantify the amount of damage that has occurred in a system. The damage metric quantification technique is not solely dedicated to the impedance method since this technique is simply a statistical method to assess the difference in two curves. Figures 4.25 and 4.26 use the damage metric technique to quantify damage.

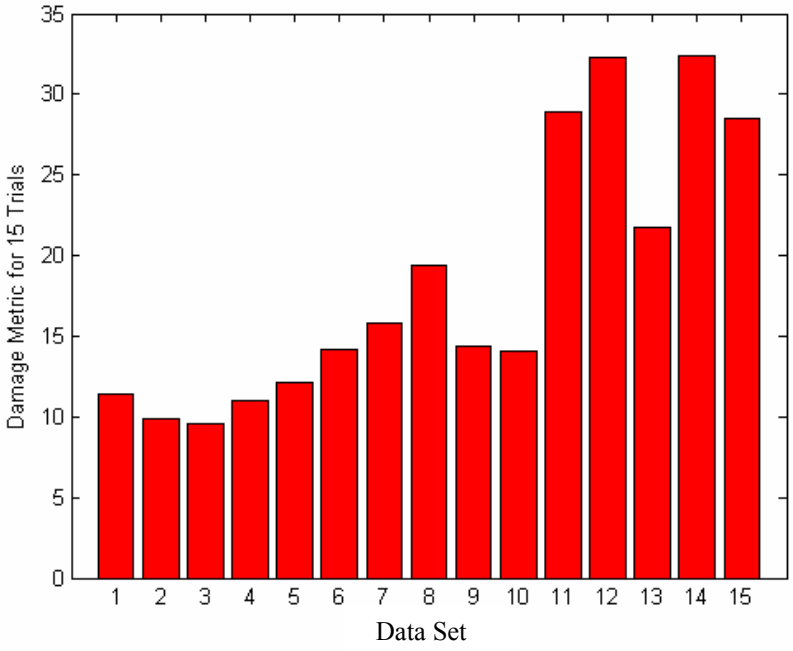

Figure 4.25. Damage metric for 15 trials of three damage cases

Note, in Figure 4.25, data sets 1 thru 5 indicate the no damage case, data sets 6 thru 10 indicate when one mass has been added at location 1 and data sets 11 thru 15 indicate when two masses have been added at locations 1 and 2. Likewise, in Figure 4.26, data sets 1, 2, and 3 are the average of the no damage case, one mass added at location 1 case, and two masses added at location 1 and 2 case, respectively.

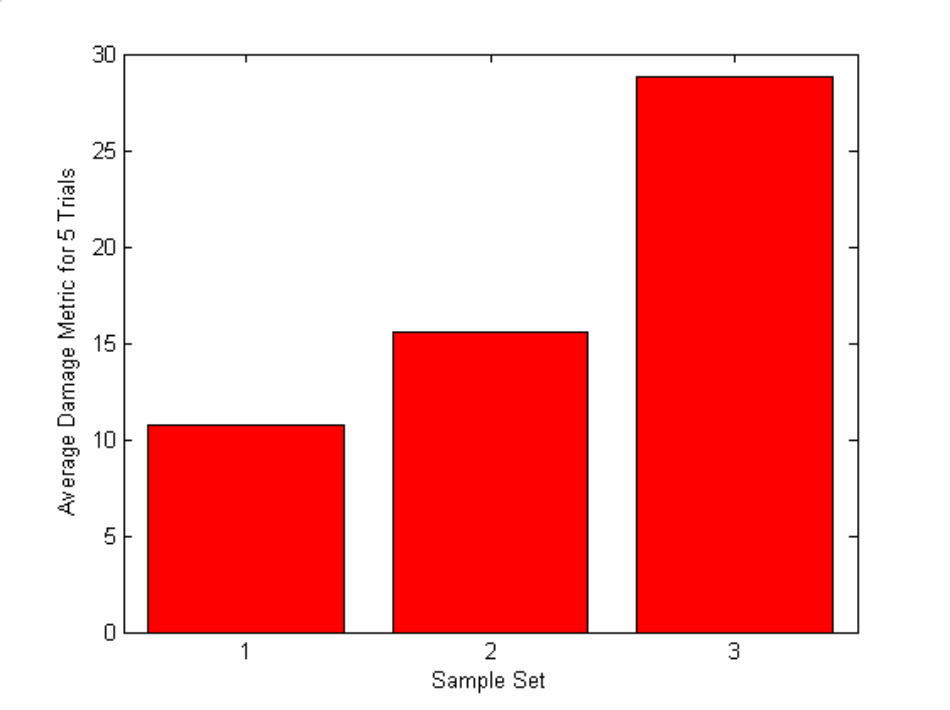

Figure 4.26. Average damage metric of 5 trials for three different damage cases

Although the results can clearly detect damage, the addition of a trigger signal to the algorithm should yield in more repeatable results. Currently, the chirp excitation signal is not starting at the same frequency for each trial. Because of this error, the structure is not excited exactly the same for each trial. As will be seen in the following section, the addition of a trigger signal to the algorithm increases the repeatable of the damage index and the damage metric values.

Results from PC 104 Board

The Prometheus PC 104 board will be discussed in greater detail in chapter 5. The Prometheus PC 104 board provides the data acquisition capabilities, memory for the baseline measurement and detection algorithm, and interface with the wireless transmitter for the CSHMS developed. The CSHMS includes the function generator board, the

wireless system, and power supply. The board uses a 100 kHz AD converter for sampling.

For this experiment, the cantilever beam was again tested but a frequency range of 3 kHz to 5 kHz was chosen. The data was captured using the CSHMS. The reasons for testing at higher frequencies is that higher frequencies are more sensitive to damage and testing at higher frequencies serves as a good transition from low frequency testing to impedance-based testing.

A section of the FRF obtained from this test in shown in Figure 4.27. The peak shown in Figure 4.27 appears to be a bending mode since it was sensitive to the addition of a mass on the neutral axis of the beam. Each FRF recorded is actually an average of 10 FRFs. This averaging is performed in the algorithm on the PC 104 board. Three baseline FRFs were recorded and are illustrated by the solid lines in Figure 4.27. All three baseline FRFs have a maximum at 4296.9 Hz. Next, one mass of 2.81 grams (one bolt and nut) was added to location 1, see Figure 4.20, and three FRFs were recorded. These three FRFs are the first set to the left of the baseline set in Figure 4.27. The maximum peak occurred at 4287.1 Hz for these three FRFs. Then the mass was moved to location 6, see Figure 4.20, and three more FRFs were recorded. The maximum peak again shifted to the left and occurred at 4267.6 Hz. Finally, an additional nut, with a mass of 1.18 grams, was added at location 6 and one more FRF was recorded. The maximum peak of this FRF was at 4257.8 Hz. This FRF is the curve furthest to the left in Figure 4.27.

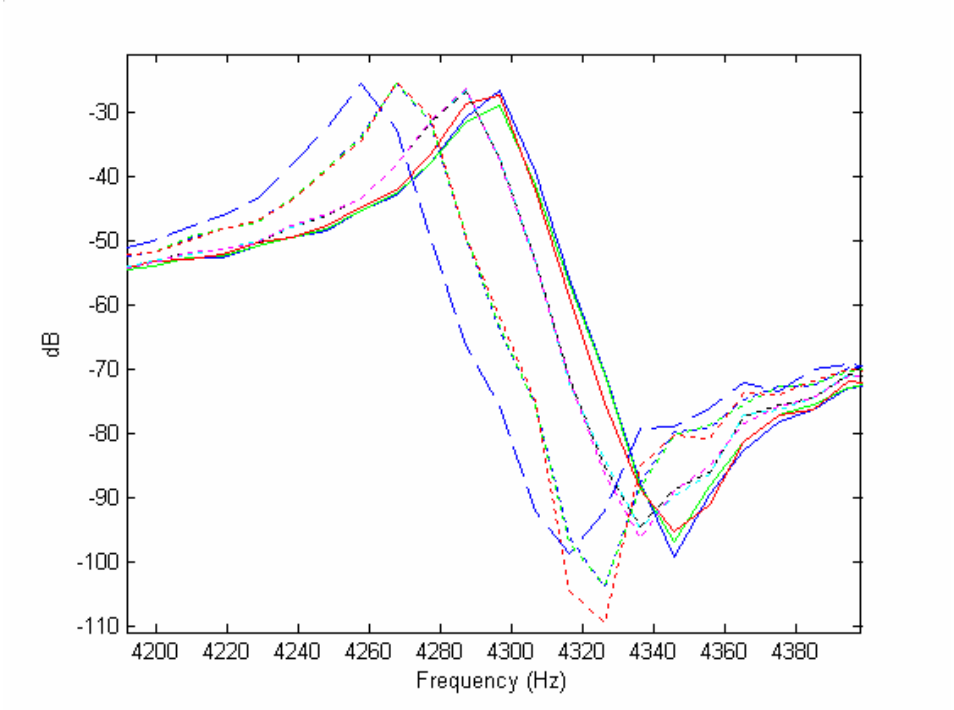

Figure 4.27. Peak of interest in FRF for the frequency shift method

Figure 4.28 was compiled by using the damage index as defined in the previous section, recall that the damage index is related to the shift in a resonant frequency with the FRF. In Figure 4.28, data sets 1, 2, and 3 represent the baseline case. Data sets 4, 5, and 6 represent the Level 1 damage case when 2.81 grams of mass (one bolt and nut) was added at location 1. Data sets 7, 8, and 9 are the Level 2 damage case when the mass was moved from location 1 to location 6 on the beam shown in Figure 4.20. Finally, data set 10 is the damage case that represents an increase in mass from 2.81 grams to 3.99 grams at location 6.

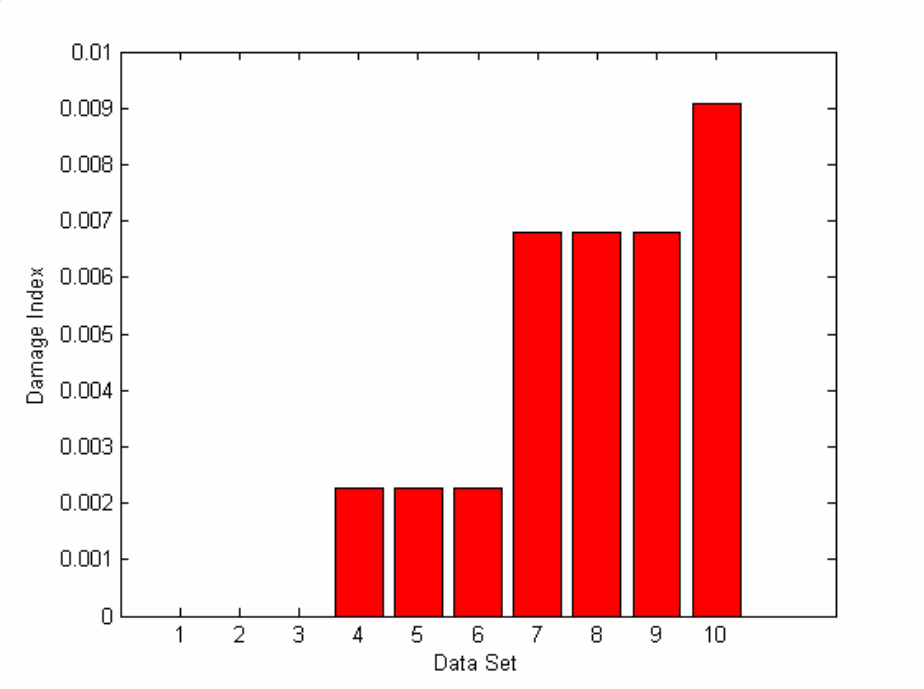

Figure 4.28. Damage index for baseline and 3 damage cases

The damage metric was also computed for FRFs shown in Figure 4.27. The metric was computed according to equation 4.1. Similar to before, the first baseline data set is considered to be data set zero and is used as the baseline for all future comparisons. Figure 4.29, shows the comparisons of sequential data sets verses data set zero, which is not shown since it was the baseline data set used for comparisons. Sets 1 and 2 are also baseline data sets. Sets 3, 4, and 5 were taken when the 2.81 gram mass was added at location 1. Sets 6, 7, and 8 were taken when the 2.81 gram mass was moved to location 6. Finally, set 10 was recorded when the mass at location 6 was increased from 2.81 grams to 3.99 grams.

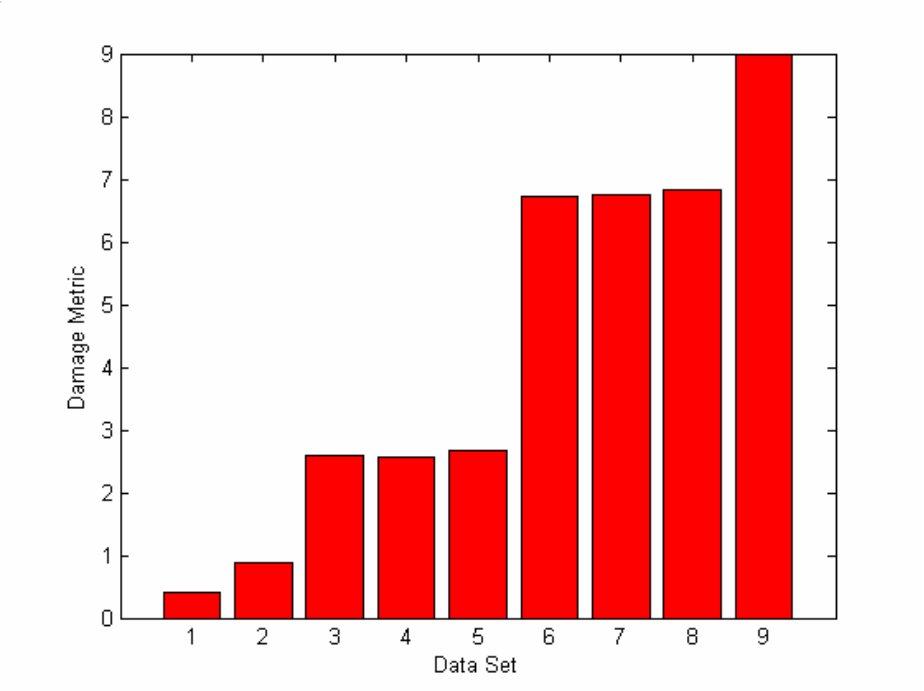

Figure 4.29. Damage metric for 3 kHz to 5 kHz beam experiment

Table 4.1. Damage index and damage metric results for the beam experiment

	Data Set 0	Data Set 1	Data Set 2	Data Set 3	Data Set 4	Data Set 5	Data Set 6	Data Set 7	Data Set 8	Data Set 9
Damage Index	-	0	0	0.0023	0.0023	0.0023	0.0068	0.0068	0.0068	0.0091
Damage Metric	-	0.4203	0.883	2.5893	2.5584	2.6676	6.7116	6.7520	6.8166	8.9876

From Table 4.1, the damage index values were constant for each damage scenario. However, the damage metric values varied within each damage scenario. Therefore, the mean and standard deviation for the first and second damage cases are reported here. The first damage case represents data sets 3, 4, and 5. The second damage case represents data sets 6, 7, and 8. The third damage case is represented in data set 9. For the baseline case, the average damage metric was 0.6516. For the first damage case, the damage metric was 2.6051 ± 0.0563. For the second damage case, the average damage metric was 6.76 ± 0.053.

4.4 Chapter Summary

Chapter 4 discusses two damage detection techniques implemented on the CSHMS. These techniques are the impedance method and resonant frequency shift method. A brief discussion regarding sampling rate and data acquisition equipment is included in the introduction of the chapter. The remaining portion of the chapter focuses on four experiments that were conducted during the course of this research. The four experiments are as follows: impedance-based testing of a composite plate using the CSHMS, impedance-base testing of an aircraft rib using a HP 4192A impedance analyzer, resonant frequency shift testing of a cantilever beam with variable mass using dSPACE, and resonant frequency shift testing of a cantilever beam with variable mass using the CSHMS.

Chapter 5

Conclusions

This thesis has presented a new structural health monitoring system developed in CIMSS that has the capacity to perform impedance-based testing. In addition to impedance-based testing, another algorithm was also developed that compares resonant frequency shifts within the frequency response function (FRF). This chapter will contain an overview of the results and contributions of this thesis. The chapter will conclude with a future work section that will present ideas for improvements to the CSHMS.

5.1 Summary of Thesis

The first chapter of this thesis laid the background for structural health monitoring. The introduction to structural health monitoring defined the goals of such systems. The classification system, expanded by Inman (2003), is introduced, which intern introduced the modern areas of interest in structural health monitoring. Next, the demand for such SHM systems in today's structures such as bridges, aircraft, and buildings is shown by the recent growth of conferences worldwide related to this field. Then a comparison between the rotating equipment and structural health monitoring field is given as foresight into the future of this industry. The literature review for this thesis concentrates on damage detection method and structural health monitoring systems. An overview of the CIMSS structural health monitoring system (CSHMS) developed is also presented in chapter 1.

The wireless system used in the CSHMS is presented in chapter 2. The chapter presents the need for wireless communication in SHM systems. The chapter then

introduced the Radiometrix® receiver and transmitter used. Finally, the chapter compares energy requirements of the Radiometrix® transmitter with transmitters used in two other structural health monitoring systems.

In chapter 3, a discussion is given about the component needed for the CSHMS. This chapter gives an overview of PC/104 boards, the low cost method for impedance measurements, and a proposed power harvesting circuit for the CSHMS. The chapter also contains a section about digital signal processors, the insight given in this section should be used in future development.

The experimental results from several damage detection tests are presented in chapter 4. Four noteworthy experiments where conducted during the course of this research. The first experiment conducted during this research looked at resonant frequency shifts in FRFs to determine if damage had occurred in the structure. This first experiment utilized dSPACE as the data acquisition system. Since dSPACE is used in rapid prototyping of digital signal processors, this approach was taken but would be abandoned later because of difficulties programming in Simulink®. The second experiment conducted also used resonant frequency shifts to detect damage; however, the data was acquired and processed on the CSHMS. Upon detection of damage, the CSHMS would send a wireless signal to a receiver across the room, which would intern cause a LED to blink indicating damage had occurred. The final two experiments were both impedance-based test. The first of the two impedance-based test involve the testing of a composite plate. The significance of this test was that the impedance data was acquired and analyzed without the help of an impedance analyzer or FFT analyzer. The other impedance-based test was performed on an actual aircraft rib provided by the United States Air Force. This test was conducted using the HP 4192A impedance analyzer. The result of this impedance testing demonstrates that higher frequency ranges for the impedance method are more sensitive to damage than lower frequency ranges.

5.2 Contributions

The primary contribution of the research present in this thesis was an impedance based structural health monitoring system that could be used to detect damage in composite and metallic structures. This system incorporated wireless technology capable of transmitting a warning signal when damage is detected in the structure. In addition, a power harvesting system is proposed which would allow the CSHMS to operate without the need to ever change batteries.

In Pearis's (2002) dissertation, he suggest in his future work section that the low cost method for impedance measurements gives way to the development of small impedance measuring devices capable of FFT analysis. He also alludes to the fact that wireless communication technology and the impedance method could be implemented to form a wireless structural health monitoring system. The research presented in this thesis satisfies Pearis's suggestion.

5.3 Future Work

Future development of the CSHMS is inevitable. This section will outline some of the author's ideas about what could be done in the near future to improve the CSHMS.

Currently, a yes or no signal is transmitted indicating whether or not damage was detected. The use of an encoder at the transmitter and a decoder at the receiver locations would make the transmission of detailed damage data a possibility. For example, if a LCD screen was added at the receiver location than the use of a decoder would allow for the level of damage to be quantified. If a damage metric threshold is set at X level of damage and the damage metric value reaches $1.5X$. Then the LCD could display a warning that the threshold has be exceeded by 50%.

The swept sine wave that is used to excite the structure was arbitrarily chosen through trial and error. Therefore, research that would relate the parameters of this wave to the A/D sampling rate would be beneficial for obtaining data with less noise. One suggestion is to adopt a step through approach similar to the impedance analyzer.

The construction of a SHM system that utilizes a DSP instead of a microprocessor would allow for faster throughput of data. In the future higher sampling rates will need to be used for extensive testing using the impedance analyzer.

The processor used for computations in the CSHMS is a traditional microprocessor, specifically a ZFx86. This microprocessor is a fixed point 16 bit processor. The use of a 32 bit DSP would increase precision and dynamic range.

Reference

Doebling, S. W., Farrar, C. R., and Goodman, R. S., 1997, “Effects of Measurement Statistics on the Detection of Damage in the Alamosa Canyon Bridge,” *Proceedings 15th International Modal Analysis Conference*, Orlando, FL, pp. 919-929.

Doebling, S. W., Farrar, C. R., and Prime, M. B., 1998, "A Summary Review of Vibration-Based Damage Identification Methods," The Shock and Vibration Digest, Vol. 30, No. 2, pp. 91-105.

Dosch, J. J., Inman, D. J., and Garcia, E., 1992, “A Self-Sensing Piezoelectric Actuator for Collocated Control,” *Journal of Intelligent Material Systems andStructures*, Vol. 3, No. 1, pp. 166-85.

Farrar, C. R., Doebling, S. W., Cornwell, P. J., and Straser, E. G., 1997, “Variability of Modal Parameters Measured on the Alamosa Canyon Bridge,” *Proc. 15th International Modal Analysis Conf.*, Orlando, FL, pp. 257-263.

Farrar, Charles, 2003, “Structural Health Monitoring Using Statistical Pattern Recognition,” A 2½ Day Short Course, Palo Alto, California

Inman, D. J., 2003. "Smart Materials in Damage Detection and Prognosis," in Key Engineering Materials Vols. 245-246 (Proceedings of the 5th International Conference on Damage Assessment of Structures (DAMAS 2003), Southampton, UK, July 1-3, 2003), Ed. by J. M. Dulieu-Barton, M. J. Brennan, K. M. Holford, and K. Worden, Trans Tech Publications Ltd., UK, pp. 3-16.

Liang, C., Sun, F. P., and Rogers, C.A., 1994. “Coupled Electromechanical Analysis of Adaptive Material System – Determination of Actuator Power Consumption and System Energy Transfer,” *Journal of Intelligent Material Systems and Structures.* V.5, pp. 21-20.

Lynch, Jerome P., 2003a, “Proceedings from Structural Health Monitoring Using Statistical Pattern Recognition,” A 2½ Day Short Course, Stanford, California

Lynch, J.P., A. Sundararajan, K.H. Law, A.S. Kiremidjian, Thomas Kenny and E. Carryer, 2003b, “Embedment of structural monitoring algorithms in a wireless sensing unit,” Structural Engineering and Mechanics, Vol. 15, No. 3, pp. 285-297.

Lynch, J.P., A. Sundararajan, K.H. Law, A.S. Kiremidjian and E. Carryer, 2003c, "Power-Efficient Data Management for a Wireless Structural Monitoring System," Proceedings of the 4th International Workshop on Structural Health Monitoring, Stanford University, Stanford, California, September 15-17, 2003, pp. 1177-1184.

Park, Gyuhue, 2000. "Assessing Structural Integrity using Mechatronic Impedance Transducers with Applications in Extreme Environments," Dissertation, Center for Intelligent Material Systems and Structures, Virginia Tech, Blacksburg, VA, April 2000.

Park, G., J.R. Wait, H. Sohn and C.R. Farrar, 2003, "Sensing System Development for Damage Prognosis," Proceedings of the 4th International Workshop on Structural Health Monitoring, Stanford University, Stanford, California, September 15-17, 2003, pp. 591-598.

Peairs, Daniel M., 2002. "Development of a Self-Sensing and Self-Healing Bolted Joint," Masters Thesis, Center for Intelligent Material Systems and Structures, Virginia Tech, Blacksburg, VA, July 2002.

Rytter, A., 1993, "Vibration based inspection of civil engineering structures," Ph. D. Dissertation, Department of Building Technology and Structural Engineering, Aalborg University, Denmark.

Salvino, L.W., D.J. Pines and N.A. Fortner, 2003, "Extracting Instantaneous Phase Features for Structural Health Monitoring," Proceedings of the 4th International Workshop on Structural Health Monitoring, Stanford University, Stanford, California, September 15-17, 2003, pp. 666-674.

Sazonov, Edward, Kerop Janoyan, and Ratan Jha, 2004, "Wireless Intelligent Sensor Network for Autonomous Structural Health Monitoring," Proceeding of the SPIE 2004 Smart Structures and Materials, San Diego, California, March 14-18, 2004

Smith, Steven W. 1999, "The Scientist and Engineer's Guide to Digital Signal Processing," Second Edition, San Diego, CA: California Technical Publishing. (See also www.dspguide.com)

Sodano, H.A., Magliula, E.A., Park, G. and Inman, D.J., 2002, "Electric Power Generation Using Piezoelectric Devices," Proceeding of the 13th International Conference on adaptive Structures and Technologies (ICAST), October 7-9th, Potsdam/Berlim, Germany.

Sodano, H.A., Gyuhae Park, Donald J. Leo, and Daniel J. Inman, 2004, "Use of piezoelectric energy harvesting devices for charging batteries," (In Progress)

Trego, A., 2003, "Installation of the Autonomous Structural Integrity Monitoring System," Proceedings of the 4th International Workshop on Structural Health Monitoring, Stanford University, Stanford, California, September 15-17, 2003, pp. 863-870.

www.radiometrix.com

www.diamondsystems.com

Vita

Luke Andrew Martin was born on May 3, 1979 to his parents Fred and Teresa Martin in Sistersville, West Virginia. Although born in Sistersville, he was raised in Weirton, West Virginia where he graduated from Weir High School in May of 1997. The following fall he embarked on his college career at West Virginia University Institute of Technology located in Montgomery, West Virginia. During his college career, Luke held internship positions at American Electric Power's John E. Amos Plant in St. Albans, West Virginia and Marathon Ashland Petroleum LLC in Ashland, Kentucky. On May 11, 2002, Luke graduated Summa Cum Laude from West Virginia University Institute of Technology and received the coveted Presidential Leadership Citation Award during commencement exercises. After graduation, he went on to graduate school at Virginia Polytechnic Institute and State University in Blacksburg, Virginia. During his first year of graduate school, Luke pursued research funding in the area of Structural Health Monitoring under the advisement of Professor Daniel J. Inman. He was particularly interested in Structural Health Monitoring after being exposed to vibration analysis techniques used to diagnosis rotating equipment during his internships. During the summer of 2003, he began his research in the field of Structural Health Monitoring. His research focused on integrating a few existing technologies to develop a wireless self-powered structural health monitoring system that would collect data from a PZT sensor, analysis this data, and transmit a wireless signal warning if damage had occurred in the structure being monitored.